Title

Distinct function of Chlamydomonas CTRA-CTR transporters in Cu assimilation and intracellular mobilization

Journal

Metallomics, 16(3)

ISSN

1756-5901

Authors

Strenkert, Daniela
Schmollinger, Stefan
Paruthiyil, Srinand
et al.

Publication Date

2024-03-12

DOI

10.1093/mtomcs/mfae013

Distinct function of Chlamydomonas CTRA-CTR transporters in Cu assimilation and intracellular mobilization

[1,2,‡]Daniela Strenkert, [1,2,‡]Stefan Schmollinger, [2,Ψ]Srinand Paruthiyil, [1]Bonnie C. Brown, [1]Sydnee Green, [3]Catherine M. Shafer, [4]Patrice Salomé, [1,r]Hosea Nelson, [5,6]Crysten E. Blaby-Haas, [2]Jeffrey L. Moseley and [1,2,4,7,8]Sabeeha S. Merchant

[1]Department of Chemistry and Biochemistry, University of California, Los Angeles, CA 90095

[2]California Institute for Quantitative Biosciences, University of California, Berkeley, CA, 94720

[3]Molecular Toxicology Inter-departmental Ph.D. program, University of California, Los Angeles, CA 90095

[4]Institute for Genomics and Proteomics, University of California, Los Angeles, CA 90095

[5]Department of Energy Joint Genome Institute, Lawrence Berkeley National Laboratory, Berkeley, CA

[6]Molecular Foundry, Lawrence Berkeley National Laboratory, Berkeley, CA

[7]Department of Molecular and Cell Biology and Plant and Microbial Biology, University of California, Berkeley, CA, 94720

[8]Lawrence Berkeley National Laboratory, Berkeley, California 94720

[‡]Present address: Department of Energy Plant Research Laboratory, Michigan State University, East Lansing, MI, 48824

[Ψ]Present address: Medical Scientist Training Program (MSTP), Washington University School of Medicine, St. Louis, MO 63110

[r]Present address: Caltech, Department of Chemistry, 1200 E California Blvd, Pasadena, CA 91125

Short title: Copper transport and storage in Chlamydomonas

One sentence summary: Regulation of Cu uptake and sequestration by members of the CTR family of proteins in Chlamydomonas

Corresponding author: Sabeeha S. Merchant (sabeeha@berkeley.edu).

Key words: SLC31A, copper recycling, algae, lysosome related organelle

ABSTRACT

Successful acclimation to copper (Cu) deficiency involves a fine balance between Cu import and export. In the green alga *Chlamydomonas reinhardtii*, Cu import is dependent on a transcription factor, Copper Response Regulator 1 (CRR1), responsible for activating genes in Cu-deficient cells. Among CRR1 target genes are two Cu transporters belonging to the CTR/COPT gene family (*CTR1* and *CTR2*) and a related soluble protein (CTR3). The ancestor of these green algal proteins was likely acquired from an ancient chytrid and contained conserved cysteine-rich domains (named the CTR-associated domains, CTRA) that are predicted to be involved in Cu acquisition. We show by reverse genetics that Chlamydomonas CTR1 and CTR2 are canonical Cu importers albeit with distinct affinities, while loss of CTR3 did not result in an observable phenotype under the conditions tested. Mutation of *CTR1*, but not *CTR2*, recapitulates the poor growth of *crr1* in Cu-deficient medium, consistent with a dominant role for CTR1 in high affinity Cu(I) uptake. On the other hand, the overaccumulation of Cu(I) (20 times the quota) in zinc (Zn)-deficiency depends on CRR1 and both CTR1 and CTR2. CRR1-dependent activation of *CTR* gene expression needed for Cu over-accumulation can be bypassed by the provision of excess Cu in the growth medium. Over-accumulated Cu is sequestered into the acidocalcisome but can become remobilized by restoring Zn nutrition. This mobilization is also CRR1-dependent, and requires activation of *CTR2* expression, again distinguishing CTR2 from CTR1 and consistent with the lower substrate affinity of CTR2.

INTRODUCTION

Copper (Cu) is an essential element for all aerobic organisms where it participates in redox reactions or reactions involving oxygen chemistry [1]. This reactivity can be harmful to intracellular macromolecules. Furthermore, the affinity of Cu ions for metal binding sites in proteins can result in their mis-metalation [2]. Therefore, cells regulate Cu content very tightly. A balance between Cu assimilation and export is one common route to maintaining cellular Cu homeostasis. The *Enterococcus hirae* system, involving a *cop* operon encoding both influx and efflux P-type ATPase transporters, is a well-studied prototype for the maintenance of Cu homeostasis in prokaryotic systems [3]. In eukaryotes, Cu is taken up in two highly conserved steps: extracellular reduction of Cu(II) to Cu(I) followed by uptake via Cu(I) specific transporters [4-10].

The prototype assimilatory Cu(I) transporter, copper transport 1 (Ctr1p), was originally discovered in yeast (*Saccharomyces cerevisiae*) with related proteins discovered in humans, plants, other fungi and algae by homology or by functional complementation of a yeast *ctr1* mutant. These transporters are called either CTR or COPT-type proteins (Copper TRansporter in prokaryotes and mammals, COPT for COPper Transporter in land plants). Typically, CTR/COPT family members have three trans-membrane helices (TM1-TM3), an N-terminal region that is rich in methionine (Met) residues, and a cysteine (Cys) rich, C-terminal region. Individual polypeptides assemble to form trimeric pores [11-14]. TM2 and TM3 contain the highly conserved motifs, MxxxM and GxxxG, respectively [15, 16]. The Met-rich motifs are extracellular and essential for Cu(I) transport activity: they bring Cu(I) to the entrance of the homotrimeric pore. The pore itself is composed of Met triads and serves to channel Cu across the lipid bilayer. After Cu sequestration through the pore, Cu(I) binds to the C-terminal Cys-rich motifs of CTR, where it is delivered to soluble metallo-chaperones for metalation of cuproproteins and intracellular distribution. The association of intracellular Cu(I) with Cu chaperones enables passive transport of Cu(I).

Where tested, the CTRs localize to the plasma membrane of eukaryotic cells and mediate high affinity Cu(I) uptake: their loss of function can lead to cell death since Cu(I) is an essential element for most aerobic life [1]. Genes encoding Cu transporters are typically transcriptionally activated in response to poor Cu nutrition, enabling Cu acquisition in such a situation [17, 18]. In mammals, a member of the CTR family of Cu transporters, Ctr1, is endocytosed and essential for Cu sequestration into Cu storage vesicles [19, 20].

The Arabidopsis (*Arabidopsis thaliana*) genome encodes six members belonging to the CTR-type family of Cu transporters (COPT1-COPT6) [21]. Of these, COPT1, COPT2 and COPT6 are plasma membrane-localized, fully rescuing the yeast *ctr1* mutant, and are involved in Cu uptake into the cell [22-25]. COPT3 and COPT5 on the other hand are members located in internal membranes and responsible for Cu(I) sequestration into intracellular storage sites (or vacuoles) [26-28]. Roles for COPT4 have yet to be defined.

The *Chlamydomonas reinhardtii* genome (Chlamydomonas) encodes four CTR/COPT members: CrCTR1 and CrCTR2, which display the classic 3 trans-membrane topology, CrCTR3, which is derived from duplication of the linked *CTR2* gene but has lost the hydrophobic trans-membrane domains, and CrCOPT1, which shows the 3 trans-membrane structure but lacks the amino-terminal region that is rich in Met and Cys residues [7]. The distinct nomenclature reflects the closer relationship of CrCTR1 and CrCTR2 to fungal proteins and COPT1 to plant proteins. The pattern of expression of the four corresponding genes in response to Cu nutrition suggests a role for the CTRs, but not for CrCOPT1, in high affinity Cu(I) assimilation [7]. Specifically, *CTR* transcripts are increased in abundance under poor Cu nutrition but reduced in the Cu excess situation. The regulation occurs at the level of transcription through associated Cu response elements (CuREs) and a transcription factor, Copper Response Regulator 1 (CRR1). CRR1 binds to CuREs through a green-lineage specific DNA binding domain. Loss of function of CRR1 results in the loss of expression of ~ 63 genes (that define the nutritional Cu regulon in Chlamydomonas), including the *CTR*s, and hence causes poor growth in Cu-deficient medium.

Chlamydomonas CTR-like proteins are conserved in other green algae but are more similar to fungal proteins as compared to the proteins found in land plants. CrCTRs contain large C-terminal and large N-terminal extramembrane domains that are not found in CrCOPT1 (which is accordingly more similar to land plant COPT proteins). Unique characteristics of CrCTR-like proteins proteins are the replacement of some of the Met-residues in the N-terminal Cu(I)-binding region by Cys-residues. Chlamydomonas *CTR1* and *CTR2* rescue the yeast *ctr1* strain underscoring their function in Cu(I) transport [7]. CTR3 is a soluble protein that lacks transmembrane domains [29]. It is possible that CTR3 may play a role in high affinity Cu uptake by recruiting Cu(I) to the assimilation pathway components, analogous to the proposed

function of the soluble FE ASSIMILATION (FEA) proteins during iron (Fe) assimilation in Chlamydomonas [30].

In previous work, we investigated Cu metabolism and homeostasis in Chlamydomonas in response to Cu nutrition [31]. Although the genome potentially encodes dozens of cuproproteins, three proteins are dominant in contributing to the Cu quota of the algal cell: plastocyanin in the chloroplast, cytochrome (Cyt) oxidase in the mitochondrion, and a ferroxidase (FOX1) involved in high affinity Fe uptake at the plasma membrane. *FOX1* expression can be repressed in Fe-replete conditions, leaving only two proteins as biomarkers of intracellular Cu status.

Plastocyanin is the most abundant cuproprotein in Chlamydomonas (which is functionally equivalent to a photosynthetic cell in plants), but in many algae its function in photosynthesis can be replaced by a heme protein, Cyt c_6. The expression of the corresponding *CYC6* gene is activated by CRR1 under Cu-deficiency [32, 33]. Accordingly, plastocyanin is on the bottom of the hierarchy for Cu distribution in Chlamydomonas, and is a sensitive indicator of intracellular Cu status. Importantly, the function of Cyt oxidase in respiration cannot be covered by any other protein and it therefore receives Cu with the highest priority: Cyt oxidase abundance is decreased only in the most severely Cu-deficient situation. On the other end of the spectrum, when Cu(I) uptake is in excess and cells over-accumulate Cu(I) species, the metal is stored in the acidocalcisome, most likely in association with Cys or related metabolites [34].

In this work, we used a reverse genetic approach to test and distinguish the functions of the Chlamydomonas CTR proteins in the context of cuproprotein assembly and Cu homeostasis. By measuring cellular Cu content chemically, monitoring individual Cu protein abundances to assess intracellular Cu status, and visualizing a key Cu(I) storage site, we conclude that CTR1 and CTR2 are both required for Cu assimilation although with different characteristics, while CTR2 is exclusively required for Cu efflux from intracellular storage sites. CTR3 is a secreted protein that appears to be dispensable under laboratory conditions.

RESULTS AND DISCUSSION

Cu uptake is impaired in the *crr1* mutant

Since the *CTR* genes are targets of the CRR1 regulon (Figure 1A), we tested a *crr1* mutant and its complemented *CRR1* strain for Cu uptake. To this end, we first grew both strains in Cu-free medium to deplete intracellular Cu stores and added 2 µM

Cu(II), provided as CuEDTA, to each culture. We collected cells 1 h before Cu(II) addition, and 0.5 and 3 h after Cu(II) addition (see Figure 1B) to measure cellular Cu content by inductively coupled plasma- tandem mass spectrometry (ICP-MS/MS). We observed that both strains have very low Cu levels following growth under Cu-deficient conditions (Figure 1C). Importantly, while Cu content increased in the complemented *CRR1* strain rapidly (0.5 h time point), the *crr1-2* mutant strain accumulated very little Cu. Indeed, the *crr1* mutant reached less than 10% of the Cu amount in the complemented *CRR1* line after 3 h in the presence of external Cu supply (Figure 1C), consistent with a role for CRR1-dependent inducible Cu uptake in Chlamydomonas, possibly via one or more of the CTR transporters [8].

Evolution of CTR proteins from Chlamydomonas

Both CTR1 and CTR2 of Chlamydomonas have an extracellular N-terminal region enriched with Cys residues, an intracellular C-terminal region with Cys and/or His motifs, and three pore-forming TM domains for Cu(I) transport characteristic of the CTR family (Supplemental Figure 1). In addition to the Cys residues that are expected to bind Cu on the extracellular side of the membrane, Mets motifs (MxxM or MxM) are also present; 5 Mets motifs in CTR1 and 6 in CTR2 (Supplemental Figure 1). In contrast, COPT1 has a relatively short N-terminal soluble region that lacks Mets motifs or Cys residues but is dominated by histidine residues (Supplemental Figure 1). Based on blastp alignments between CTR3 and the N-terminal regions of CTR1 and CTR2, we identified 2 separate Cys-rich regions in CTR1 and CTR2, with 3 such regions in CTR3 (Supplemental Figure 1). Based on percent identity, CTR3 is likely a duplication of the N-terminal region of CTR2 followed by a tandem duplication of region 2 within CTR3. Each identified region is predicted to fold into separate structural domains, with proline-rich regions separating the two domains in CTR2 and the three domains in CTR3 (Supplemental Figure 1). Based on this analysis, we have named this conserved domain the CTRA (CTR-associated) domain and refer to this subfamily of CTRs as the CTRA-CTR proteins.

A sequence similarity network (SSN) of CTR proteins (based on presence of IPR007274) and CTR3-like proteins (based on a jackhmmer search) reveals multiple major proteins clusters that are separated largely in accordance with taxonomy (Figure 2A). Chlamydomonas COPT1 and other closely related green algal CTR proteins are connected to the land plant CTRs, which are further divided into two subclusters, represented by AtCOPT5 and AtCOPT1 (Figure 2A). Two exceptions to the

congruence between taxonomy and protein clusters are present. One cluster contains the CTR1/CTR2/CTR3 proteins from Chlamydomonas together with other green algal proteins, fungal proteins from Fungi *incertae sedis*, and proteins from Amoebozoa. The second cluster contains proteins from an assortment of lineages, including green algae and various protists. The protist cluster contains proteins from several Chlamydomonas species, but not *Chlamydomonas reinhardtii*. The CTR1/CTR2/CTR3 cluster contains a mix of stand-alone CTR3-like proteins and CTR proteins that contain one or more CTRA domains (Figure 2A).

This analysis also reveals that fusion proteins involving CTR are not unique to CTR1/CTR2. Five other types of N-terminal extensions involving annotated domains are present, as well as five types of C-terminal extensions (Supplemental Figure 2). Metal-related examples are the C-terminal HMA (Heavy Metal Associated) domains found in the protist cluster and the C-terminal BIM1 domains previously identified in *Cryptococcus neoformans* [35]. Small soluble proteins containing the HMA domain often function as Cu chaperones and are proposed to acquire Cu directly from CTR [36], while BIM1 is involved in Cu acquisition [35]. Since this analysis relies on identification of annotated domains, undescribed domains in addition to the CTRA domains found in CTR1/CTR2/CTR3 likely exist. One example is the unannotated N-terminal domain found in the protist cluster, represented by CTR protein from the oomycete *Albugo candida* (Supplemental Figure 2), which is also found as a stand-alone protein in other protists and green algae but is not related with the CTRA domain. Although this type of CTR fusion protein is not found in *Chlamydomonas reinhardtii*, the stand-alone protein is conserved (Cre05.g236039) and is a target of CRR1, suggesting that this uncharacterized protein may function in Cu acquisition.

Phylogenetic reconstruction of CTR1, CTR2, CTR3 and similar proteins confirms the relatedness of these proteins to CTRA-CTR proteins from Fungi *incertae sedi*s and Amoebozoa. The phylogenetic tree suggests that a geen algal ancestor that existed before the split of Pedinophyceae, Chlorophyceae, and Trebouxiophyceae could have acquired a CTRA-CTR fusion protein from an ancestor of the Chytridiomycetes. Chytridiomycetes are typically known as aquatic parasites and can infect green algae, but some species form a facultative mutualistic relationship with green algae [37]. The evolution of CTR3, likely resulting from a partial duplication of the ancestral *CTR2*, appears to have occurred in an ancestor of the Chlamydomonadales. There is also

evidence of independent duplications leading to the evolution of CTRA-containing proteins that lack the CTR TM helixes (Figure 2B).

Biochemical fractionation indicated plasma membrane localization for CTR1 and CTR2, suggesting that one or both proteins might function *in vivo* in Cu(I) transport [7]. By contrast, CTR3 was previously detected in soluble fractions of cells rather than in the membrane, consistent with the absence of TM domains in this protein [29]. We asked whether CTR3 might be a secreted protein, in a manner analogous to the periplasmic FEA proteins suspected to be involved in Fe assimilation [30], by monitoring CTR3 abundance in the spent medium of a cell-wall deficient (*cw*) strain (Supplemental Figure 3). A protein that is located to the periplasmic space is lost to the medium in a *cw* strain. Proteins in the spent medium were concentrated (e.g. by acetone or trichloroacetic acid (TCA) precipitation (Supplemental Figure 3A)), separated by SDS-PAGE and analyzed by immunoblotting with an antibody raised against CTR3. We detected the presence of CTR3 only in the spent medium of *cw* cultures under Cu-deficient conditions independent of how we precipitated proteins in the spent medium (Supplemental Figure 3). We validated the Cu status of the cells by immunoblotting for Cox2b (lower abundance in low Cu). We also detected FEAs in the spent medium. We conclude that CTR3 is likely not a transporter, nor does it have strong, stable association with a plasma membrane–localized protein (e.g. CTR1 or CTR2) to be retained by *cw* cells. Our results suggest that CTR3 is therefore either a periplasmic protein or associated with a cell wall component (see conclusions).

Reverse genetics to assess the function of each member of the Chlamydomonas CTR family

To directly assess the function(s) of individual CTR proteins in Chlamydomonas, we generated or identified candidate loss of function mutants. For *CTR1*, we used CRISPR/Cpf1-based gene editing [38-40] (see Methods), while for *CTR2* and *CTR3*, we obtained candidate loss of function insertion mutants from the Chlamydomonas Library Project, CLiP [41]. We introduced two in frame stop codons within the first exon of the *CTR1* gene (Supplemental Figure 4A, white filled arrow). From 178 transformants screened, we identified five independent lines, named *ctr1-1* through *ctr1-5*. Sequencing of the PCR-amplified product spanning the gene editing site confirmed the presence of the two stop codons in all five *ctr1* lines, with *ctr1-2* harboring an additional insertion of three in frame codons (Supplemental Figure 5). Molecular analysis of *ctr1* lines indicated the absence of *CTR1* transcripts (Supplemental Figure

4B) and the absence of the corresponding polypeptide (Supplemental Figure 4C). For *CTR2* and *CTR3*, we confirmed disruption of the loci by PCR and Sanger sequencing. While *ctr2-1* has an insertion in the second exon of *CTR2* and a complete loss of *CTR2* mRNA, we noted that *ctr2-2* has an insertion in the second intron and expresses a low, but detectable, amount of the *CTR2* transcript (Supplemental Figure 4B, 3.2%). Immuno-detection confirmed that *ctr2-2* is a weak allele with a small amount of residual protein (Supplemental Figure 4D). For *CTR3*, genotyping confirmed the location of the insert in *ctr3-1*, and qRT-PCR and immunodetection, respectively confirmed the absence of mRNA and protein (Supplemental Figure 4B and C).

CTR1 and CTR2 mediate Cu uptake in Cu replete cells

We measured the Cu content of each mutant and corresponding wild-type strains (CC4533 for insertion mutants; *CTR1* for *ctr1* mutant strains) in medium containing sufficient (2 µM) but not excess Cu [31]. For *ctr1*, the Cu content reached 77% of wild-type levels (Figure 3A, shown is the average and individual data points of all five allelic strains). Likewise, both the null *ctr2-1* strain and the weak allele (*ctr2-2)* had less Cu compared to the wild-type, with *ctr2-1* showing a stronger decrease with respect to Cu content (66% of wild-type levels) than *ctr2-2* (77% of wild-type levels) (Figure 3A). We conclude that CTR1 and CTR2 both contribute to Cu assimilation in Cu-replete conditions. When we monitored the abundance of *CTR1* and *CTR2* transcripts in the mutants, we observed a dramatic 46-fold increase in *CTR2* transcripts in the *ctr1* mutants, and a smaller ~ 3-fold increase for *CTR1* transcripts in the *ctr2-1* mutant and up to 2-fold increase in *ctr2-2* (Figure 3B). Thus, the absence of either transporter triggers induction of the Cu assimilation machinery, albeit to different degrees. In both cases, the induction of one transporter gene does not fully compensate for the loss of the other, speaking to distinct functions for CTR1 and CTR2.

We hypothesized that the observed increase in *CTR1* transcripts in *ctr2* cells under classic Cu-replete conditions (and *CTR2* transcripts in Cu-replete *ctr1* cells) relative to wild-type cells may reflect an intracellular Cu deficiency, which would lead to the activation of the CRR1 regulon. We tested this hypothesis by immunoblot analysis with the Cu deficiency marker Cyt c_6. Indeed, we detected Cyt c_6 in both *ctr2* mutants grown in TAP medium with 2 µM Cu (Cu-replete condition) (Figure 4AB) with the level of Cyt c_6 accumulation proportional to the magnitude of the Cu deficiency. By contrast, the *ctr1-1* mutant strain showed no evidence of internal Cu deficiency, as evidenced by the absence of Cyt c_6 under Cu-replete conditions (Figure 4A), suggesting that another

mechanism is responsible for the compensatory increase of *CTR2* transcripts in the *ctr1* strain. How the changes in transcript levels translate to the abundance of the corresponding transporters, if any, has not been determined.

Loss of CTR1 or CTR2 results in stronger phenotypes in Cu deficiency

Despite the lower Cu content of *ctr1* and *ctr2* mutants, we noticed no effect on their growth relative to the corresponding wild-type strains in Cu-replete conditions (Figure 5, Supplemental Figure 8). We therefore tested the mutants for growth in Cu-deficient medium when both genes are normally induced (Figure 5B, Supplemental Figure 6). The *ctr2* and *ctr3* strains had doubling times comparable to those of the corresponding wild-types, about 8 h in Cu-replete medium, with doubling times for *ctr2* mutant strains appearing to lag behind that of the wild-type, although this difference did not reach significance (Supplemental Figure 6). In sharp contrast, the *ctr1* strains were unable to grow in Cu-deficient medium recapitulating the *crr1* growth phenotype (Figure 5B). When we tested the *ctr1* strains for the accumulation of sentinel proteins for intracellular Cu status, plastocyanin and Cyt c_6, we noted a normal pattern of Cu nutrition-dependent accumulation for plastocyanin and Cyt c_6, indicating that the CRR1 regulon functions properly in the *ctr1-1* mutant (Figure 4). This observation suggests that the very poor growth displayed by *crr1* may be attributed to the lack of induction of *CTR1* in Cu-deficient conditions (Figure 5B). The *ctr2* strains also showed wild-type accumulation of plastocyanin and Cyt c_6 in Cu-deficient medium, confirming, together with the absence of a growth phenotype, successful acclimation to Cu deficiency (Figure 4B). The *ctr2-1* strain, which is more Cu-deficient, accumulated more Cyt c_6 than did the *ctr2-2* strain in Cu replete conditions, relating the severity of the phenotype to the severity of the genetic lesion.

We conclude that the phenotypes of the *ctr1* and *ctr2* strains under poor Cu nutrition are distinct and this observation reinforces the notion that they have non-redundant roles in Cu homeostasis.

Distinct functions of CTR1 and CTR2 in high- and low-affinity Cu uptake

To directly assess the function of CTRs in Cu(I) uptake, we measured the total cellular Cu content of Cu-deficient cells by ICP-MS/MS either before (-1 h, to establish the ground state) or after (+0.5 h and 3 h) addition of 100 nM Cu to probe high-affinity uptake. We also tested low-affinity Cu uptake by performing the same experiment with the addition of 2 µM Cu (Figure 6). With the addition of 2 µM Cu, the Cu uptake of the *ctr1* and *ctr3* mutants was indistinguishable from that of their corresponding wild-type

reference strains (Figure 6A and Supplemental Figure 7). Notably, the two *ctr2* mutant strains showed poor uptake kinetics (Figure 6D). Even at 3 h after addition of 2 μM Cu, the Cu content of the *ctr2-1* and *ctr2-2* strains was only 14% and 20% of the wild-type, respectively, indicating that CTR2 is responsible for a large portion of the Cu assimilated at higher extracellular Cu concentrations. This result is consistent with the apparently normal Cu uptake seen in the *ctr1* mutant strains at high extracellular Cu, with Cu uptake occurring through CTR2. When we assessed high-affinity transport with the addition of 100 nM Cu, the *ctr1* mutants had 10-fold less Cu than the corresponding wild-type (Figure 6B), explaining its poor growth in Cu-deficient conditions (Figure 5B). The *ctr2* mutants accumulated Cu, albeit less than the wild-type (Figure 6E). We speculate that the slower but continuous accumulation of Cu in the *ctr2* strains growing in the presence of 100 nM Cu, presumably through CTR1, allows growth of *ctr2* in Cu-deficient medium, and indicates that CTR1 contributes predominantly to high-affinity Cu uptake.

The distinct outcome from the addition of 100 nM Cu or 2 μM Cu to the *ctr1* cultures suggests that CTR1 is a high-affinity Cu transporter, while CTR2 may be important for low-affinity Cu transport. We conclude that CTR2 cannot rescue *ctr1* in low Cu despite a striking ~ 30-fold increase in *CTR2* transcript levels in the *ctr1* mutant strains (Figure 6C); under high Cu conditions, CTR2 can compensate for the loss of CTR1. CTR1, conversely, can rescue the *ctr2* mutants in medium containing low Cu, but not high Cu, and *CTR1* transcripts are also not increased in abundance in Cu deficient *ctr2* mutants (Figure 6F). This anomaly can be explained if CTR1 does not function when Cu content in the growth medium is high. For instance, CTR1 may be removed from the plasma membrane by ubiquitylation and degradation or by endocytosis [42]. The results of the above experiments highlight the distinct molecular properties of CTR1 and CTR2 *in vivo*: CTR1 is most relevant when Cu availability is low, while CTR2 is more relevant when Cu concentrations are higher.

CTR transporters are responsible for luxury Cu uptake in Zn-deficient cells

Zn is another element that is required at trace levels for all forms of life because of its function as an electrophile. Like Cu, it is at the top of the Irving-Williams series and binds tightly to functional groups found in proteins. Metabolic connections between Cu and Zn have been observed in some organisms, and in general the molecular basis for these connections is not known [43-45]. We determined that *crr1* cells are more compromised for growth in Zn-deficient medium compared to the complemented *CRR1*

strain (Supplemental Figure 8), suggesting a role for CRR1 in low Zn conditions. When we tested individual *ctr* mutants to assess whether loss of CTR function might be responsible for the *crr1* phenotype in Zn-deficient conditions, we observed that none of the *ctr* strains show a growth phenotype similar to that of *crr1* (Supplemental Figure 8) even though the abundance of *CTR* transcripts increases in Zn-deficient cells (Figure 7A). We conclude that the poor growth of Zn-deficient *crr1* strains cannot be attributed to loss of *CTR* expression. The magnitude of the increase in *CTR* expression in Zn-deficient wild-type cells is smaller than that in Cu-deficient cells, but it is significant and it correlates with unusually high Cu content in Zn-deficient cells [46]. The accumulation of unusually high amounts of Cu is unique to Zn deficient cells, as Zn replete cells don't accumulate Cu higher than their typical quota [7, 46].

We tested each *ctr* mutant individually for its contribution to Cu accumulation under Zn deficiency (Figure 7). The *ctr1* and *ctr2* mutants accumulated less Cu compared to the corresponding wild-type strains, specifically when Cu was supplied at a range of 0.2 µM to 2 µM in the growth medium, with *ctr1* displaying a stronger phenotype, compatible with the model that CTR1 is the higher affinity transporter. When Cu concentrations in the medium were increased to 10 µM or 20 µM, Cu accumulation in *ctr1* matched that in the wild-type (Figure 7B, C). This finding raised the possibility that excess Cu in the medium might allow *crr1* mutants to grow under Zn deficiency and might also allow this mutant to overaccumulate Cu so that we could assess whether CRR1 has an impact on Cu mobilization from intracellular stores (see below).

Nutritional complementation of the *crr1* mutant with Cu distinguishes Cu transport into and out of the acidocalcisome

We designed a strategy to force Cu uptake into the Zn-deficient *crr1* mutant. Because *crr1* grows poorly under prolonged Zn-deficient conditions, we first grew *crr1* and *CRR1* strains in medium replete for Zn and Cu (where the mutant grows well) and collected 2×10^8 cells, which were washed twice with 1 mM EDTA to remove bound metals from the cell surface before dilution into fresh Zn-deficient medium to a final cell density of 2×10^6 cells/mL for each strain (comparable to a log phase culture). To drive Cu into the *crr1* mutant (which cannot up-regulate the *CTR*s), we supplied the Zn-deficient *crr1* culture with the maximum amount of Cu (40 µM) the cells could tolerate (Figure 8AB), to effect Cu over-accumulation (which was less than what is commonly observed in Zn deficient wild-type cells in standard 2 µM Cu medium). To match this moderate intracellular Cu accumulation in the comparison Zn-deficient *CRR1* culture, we reduced

Cu supplementation to 1.2 µM. This protocol allowed growth of the *crr1* mutant in Zn deficiency for 2 days with Cu accumulation in *crr1* comparable to that in the wild-type *CRR1* strain after dilution into Zn-deficient, Cu-excess conditions (Figure 8C). This allowed us to analyze the requirement for CRR1 in intracellular Cu distribution and to distinguish the roles of CTR1 and CTR2.

In wild-type cells, excess Cu localizes to the acidocalcisome, a low-pH compartment containing polyphosphate and calcium ions (Ca^{2+}) [46]. When we stained cells with the Cu dye Coppersensor-3 (CS3) to visualize Cu(I) storage sites, we detected distinct foci in the *crr1* and *CRR1* strains after transfer to Zn-deficient medium (Figure 8D). We conclude that excess external Cu can bypass the requirement for CTR transporters for Cu uptake into cells during Zn deficiency. The subsequent Cu sequestration into the acidic vacuoles occurs independently of CRR1 and CTRs. To test whether this sequestered pool of Cu can be remobilized, we supplied cultures with 2.5 µM Zn (to restore the Zn-replete condition): we noticed the release of Cu from vacuoles in the *CRR1* strain within 7 h, in agreement with previous results [46] but not from the *crr1* mutant (Figure 8D and Supplemental Figure 9). We conclude that the transporter responsible for efflux of Cu(I) from the acidocalcisome is a target of CRR1.

We investigated the possible contribution of each Cu transporter to Cu efflux from the acidocalcisome by probing each *ctr* mutant for mobilization of stored Cu(I) from the acidocalcisome. The *ctr* mutants accumulated Cu to a moderate level when grown under Zn deficiency with standard 2 µM Cu supplementation (Figure 7B, C): the accumulated Cu(I) was visible as distinct foci corresponding to the acidocalcisomes (Figure 9 upper panel), similar to wild-type strains and the *crr1* mutant. We conclude that none of the transporters is likely required for sequestration into acidocalcisomes. However, upon re-supply of Zn, only the *ctr1* and *ctr3* mutant strains were able to mobilize Cu(I) from the organelle, while Cu(I) foci remained in both *ctr2* mutants (Figure 9 lower panel and Supplemental Figures 10 and 11). We conclude that CTR2 may localize, at least in part, to the boundary membrane of the acidocalcisome and functions to release Cu(I) from intracellular stores. The concentration of Cu(I) in the acidocalcisome is expected to be high in the Cu-accumulating situation driven by Zn deficiency, which is compatible with the lower substrate affinity of CTR2 for Cu(I).

CONCLUSIONS

A previous study revealed that Chlamydomonas, like many other organisms, contains more than one gene encoding CTR-type Cu transporters [7]. COPT1 is most closely

related to Arabidopsis Cu transporters but its expression is unchanged in response to Cu nutritional changes and its heterologous expression does not rescue the yeast *ctr1* mutant [7, 21]. In this work, we establish CTR1 and CTR2 as members of the phylogenetically distinct CTRA-CTR family and as canonical Cu transporters *in vivo*.

CTR1 and CTR2 are likely the descendants of a CTRA-CTR protein acquired from a Chytrid, which functionally replaced the laterally inherited plant-like CTR protein for Cu assimilation across the plasma membrane. Presumably, the Cu-acquisition characteristics enabled by the presence of the CTRA domains (that are shared with extant Chytrids) provided a selective advantage over the ancestral plant-like CTR protein. Another selective advantage acquired during the evolution of the Chlamydomonadales was enabled by the evolution of a secreted protein containing three CTRA domains. However, the selective advantage due to the presence of CTR3 and similar proteins has yet to be elucidated. The predicted N-terminal signal sequence is compatible with secretion where it may reside in the periplasmic space or associate with extracellular cell wall components. The latter is unlikely, given that CTR3 was reliably quantified by mass spectrometry in soluble fractions from cell walled Chlamydomonas [29]. A CTRA-containing protein, analogous to CTR3, has evolved independently in the amoeba *Dictyostelium discoideum* likely after duplication of the gene encoding the CTRA-CTR protein referred to as P80 [47]. However, whereas CTR3 has three CTRA domains, the soluble P80-derived protein has a single CTRA domain. P80 and orthologous CTRA-CTR proteins from Amoebozoa are likely also the descendants of a horizontally transferred gene from an ancient Cytrid, but the event was independent from the event that resulted in the green algal CTRA-CTR proteins. Although we could not distinguish a phenotype for loss of function of soluble CTR3 in Chlamydomonas, the multiple independent evolution of such forms speaks to its relevance.

Conservation of the putative Cu-binding ligands in the fungal, amoeba, and algal CTRA-CTR and stand-alone CTRA proteins suggests that the CTRA proteins play a role in Cu homeostasis, possibly in Cu acquisition prior to transport by CTRA-CTR. However, under the conditions tested here, we did not observe a Cu-assimilation defect in the CTR3 mutant. Based on the presence of characterized and uncharacterized proteins in the CRR1 regulon, *C. reinhardtii* has acquired an arsenal to compete with other organisms for Cu and thrive during Cu limitation. As such, there may be several functionally overlapping pathways that can complement the loss of

CTR3. One such pathway may involve Cre05.g236039, an unrelated, soluble protein predicted to be secreted, that contains numerous Cys, Met, and His residues. Like CTR3, orthologs of Cre05.g236039 are often fused to the N-terminus of CTR proteins in other algae and protists. The reason why some green algae employ the CTRA-CTRs, while others employ the Cre05.g236039-like-CTR fusions is unknown, but the presence of CTR3, Cre05.g236039 and possibly other putative, extracellular, Cu acquisition proteins points to the presence of a complex, seemingly redundant Cu-acquisition strategy.

In the case of Cu transport across the plasma membrane, our results presented here highlight the distinct functional roles of the paralogs CTR1 and CTR2. Retaining horizontally transferred genes and duplication events giving rise to multiple CTR paralogs with different functional properties has likely enabled Chlamydomonas and other organisms to fine-tune Cu uptake and distribution. In particular, differences in domain organization, even relatively minor differences in Cu-binding motifs, allow for functional flexibility in Cu assimilation. CTR1 functions as a high-affinity importer whose activity is turned off at high extracellular Cu to prevent Cu overload during transition of cells from very low to high Cu. This could occur by ubiquitylation followed by endocytosis or degradation. CTR2 has two functions: it enables Cu(I) uptake but only at high Cu content in the medium and is a lower affinity transporter that delivers Cu(I) to the cytoplasm from intracellular stores where the Cu(I) content is high. The latter is consistent with CTR2 being identified in isolated acidocalcisomes by mass spectrometry [48]. The combination of transporters with different affinities, localization and trafficking allows tight control of cytoplasmic Cu availability for cuproprotein synthesis. Our study represents the first step in understanding CTR-type Cu transporters in the green algae, and paves the way for future functional dissection of their Cu-dependenttrafficking, localization and degradation.

Chlamydomonas' Cu quota is determined by the abundance of its cuproproteins with little or no pools of exchangeable Cu species [49]. When cells lack Zn, Cu homeostasis is disrupted, possibly because CRR1 function is not turned off, the CTRs are expressed, and Cu accumulates up to 40-fold of its usual quota [46, 50]. The excess Cu can be especially deleterious when Zn is low because protein mis-metalation might become common as cuprous and cupric ions are competitive with Zn for metal binding sites in proteins [51]. Cu sequestration via compartmentation is nature's solution to this problem. Most eukaryotes evolved systems that allow Cu sequestration into

compartments if Cu is available in excess (into vacuoles or acidocalcisomes) but also ensure that stored Cu may be accessed at a later time if needed. In this work, we exploited the Zn deficiency induced disturbance of Cu homeostasis to show that the mobilization of Cu from the acidocalcisomes is mediated by CTR2 in Chlamydomonas.

METHODS

Generation of ctr1 KO strains using CRISPR/Cpf1

CC-425, a cell wall reduced arginine auxotrophic strain, was used for transformation with a ribonucleoprotein (RNP) complex consisting of a guide RNA (gRNA) targeting a PAM sequence in exon1 of *CTR1* and LbCpf1 as described in [38, 40]. Modifications are outlined as follows: cultures were grown to 2 x 10^6 cells per mL and counted by using a hemocytometer. For optional pretreatment, 2 x 10^7 cells were suspended and centrifuged (5 min, 1424 x*g*) in Maxx Efficiency Transformation Reagent (1 mL) twice, followed by suspension in 230 µL of the same reagent supplemented with sucrose (40 mM). Cells were incubated at 40°C for 20 minutes. Purified LbCPF1 (80 µM) was preincubated with gRNA (1 nmol, targeting sequence = TTTGGGATGCGGCGGCGCTCAGCGG) at 25 °C for 20 min to form RNP complexes. For transfection, 230 µL cell culture (5 × 10^5 cells) was supplemented with sucrose (40 mM) and mixed with preincubated RNPs and *Hin*DIII digested pMS666 containing the *ARG7* gene conferring the ability to grow without arginine. CC-425 transformed with *ARG7* was used to generate reference strains (*CTR1*). In order to achieve template DNA-mediated editing, an ssODN containing two stop codons after the PAM target site (~4 nmol, sequence = GTAGCTACTGACGTGTGCAGCTCGTTCATTTGGTAAGCGTAGGCGCTCAGCGG CTACTGCACGACGACCGGCGCTCTGGCGTACCGGTCG) was added. The final volume was 280 µL. Cells were electroporated in a 4-mm gap cuvette (Biorad) at 600 V, 50 µF, 200 Ω using a Gene Pulser Xcell (Bio-Rad). Immediately after electroporation, 800 µL of TAP with 40 mM sucrose was added. Cells were recovered overnight in darkness and without shaking in 5 mL TAP with 40 mM sucrose and polyethylene glycol 8000 0.4% (w/v) and then plated on TAP after a 5 min centrifugation at RT and 1424 x*g* using the starch embedding method. Since we did not expect a phenotype, colonies were screened by qPCR for successful genome editing at the *CTR1* locus. Colony qPCR of transformants was performed as follows: after one week of growth, half of each colony on TAP plates was resuspended in 50 uL 10 mM Tris-HCl (pH 8) buffer in a 96 well plate. Cells were heated to 96 °C for 10

min. After vortexing, 96 well plates were spun down for 4 min at ~1000 x*g*. Supernatants containing the DNA were transferred to new 96 well plates. qPCR on a total of 178 clones was performed using oligos Ctr1screenfor CAGCTCGTTCATTTGGGATG (which was specific for the wild-type, unedited *CTR1* gene) and Ctr1unirev GTGTGAGAGCTGGCTGATCC. The following program was used for all qPCR reactions: 95°C for 5 min followed by 40 cycles of 95°C for 15 s, and 65°C for 60 s. 11 clones failed to amplify the wild-type CTR1 sequence; these were subjected to a secondary screen using oligo Ctr1seqfor ACGTGTGCAGCTCGTTCATT (specific for gene-edited *ctr1* alleles) and Ctr1unirev GTGTGAGAGCTGGCTGATCC. Sequencing of the PCR products using oligo Ctr1unirev revealed that 5 clones had ssODN-mediated gene editing within the first exon of CTR1, and all of them showed successful introduction of the two stop codons. *ctr1-3* also contained three extra base pairs integrated downstream of the gene editing target site in addition to the two stop codons in exon1 (Supplemental Figure 1).

Culture conditions and additional Chlamydomonas strains

Insertional mutant lines from the Chlamydomonas Library Project (CliP) [41] were designated as *ctr2-1* (LMJ.RY0402.151308), *ctr2-2* (LMJ.RY0402.163662), *ctr3-1* (LMJ.RY0402.179604). The mutants and corresponding wildtype strain CC4533 were genotyped by PCR and amplicons were sequenced to confirm predicted integration of the insertion cassette. The *crr1* mutants (CC5068) and *crr1* lines complemented with *CRR1* genomic sequence (CC5070, designated as *CRR1*) were characterized previously [52, 53]. Unless stated otherwise, cells were grown in Tris-acetate-phosphate (TAP) with constant agitation in an Innova incubator (160 rpm, New Brunswick Scientific, Edison, NJ) at 24°C in continuous light (90 µmol m-2 s-1), provided by cool white fluorescent bulbs (4100K) and warm white fluorescent bulbs (3000 K) in the ratio of 2:1. Cell wall reduced strains CC425 were grown under the same light regime but with constant agitation at 140 rpm. TAP medium with or without Cu or Zn was used with revised trace elements (Special K) instead of Hunter's trace elements [54].

Precipitation of secreted proteins

Cells from strain CC5390 were analyzed after three rounds of growth in Cu-deficient TAP medium to stationary phase. Cells were collected by centrifugation at 4°C for 10 min at 1424 x*g*. Following centrifugation, pellets were resuspended in a lysis solution (125 mM Tris-HCl pH 6.8, 20% glycerol, 4% SDS, 10% β-mercaptoethanol, 0.005%

bromophenol blue). After a second centrifugation at 4°C for 10 min at 4000 rpm, the supernatant was filtered through a 0.4-µm filter before ice-cold 100% trichloroacetic acid (TCA) was added to the samples to a final concentration of 10%. Samples were mixed and incubated overnight at 4°C. The samples were then centrifuged at 4°C for 10 min at 1424 x*g* and resuspended in ice-cold acetone. Another centrifugation at 4°C for 10 min at 1424 x*g* was performed before final protein pellets were resuspended in 2 x sample buffer (125 mM Tris-HCl pH 6.8, 20% [v/v] glycerol, 4% SDS, 10% β-mercaptoethanol, 0.005% bromophenol blue) and incubated for 10 min at 65°C before storage at –80°C.

Antibody production and protein analyses by immunodetection

Antibodies against CTR1 were produced by COVANCE via immunization using the subcutaneous implant procedure of rabbits following a 118-day protocol with synthetic peptide Ac-CNAKARRGSGDALGANTADHKKGASS-amide. For analysis of total proteins, 15 mL of a Chlamydomonas culture with a cell density of 4-8 x 10^6 cells/mL was centrifuged for 3 min at 4°C and at 1650 x*g*. The resulting cell pellet was resuspended in 300 µL of a buffer containing 10 mM Na-phosphate buffer (pH 7.0), EDTA-free Protease inhibitor (Roche), 2% (w/v) SDS, and 10% (w/v) sucrose. For analysis of soluble and membrane fractions, 15 mL of a culture at a cell density of 4-8 x 10^6 cells/mL was centrifuged at 1650 x *g*. The cell pellet was resuspended in 300 µL of buffer containing 10 mM Na-phosphate buffer (pH 7.0) and EDTA-free Protease inhibitor (Roche). Soluble and membrane fractions were isolated by lysing cells with three freeze-thaw cycles (−20°C to room temperature). After lysis, soluble proteins (supernatant) were separated from the membrane bound proteins (pellet) by centrifugation at 4°C. Membrane-bound proteins were resuspended in 200 µL Na-phosphate buffer containing 2% Triton X-100 before both fractions were quick-frozen in liquid N_2. Samples were stored at −80°C prior to analysis. Protein amounts were determined using a Pierce BCA Protein Assay Kit against BSA as a standard and diluted with 2 x sample buffer (125 mM Tris-HCl pH 6.8, 20% [v/v] glycerol, 4% [w/v] SDS, 10% [v/v] β-mercaptoethanol, 0.005% [w/v] bromophenol blue). Proteins were separated on SDS-containing polyacrylamide gels using 10 µg of protein per lane. The separated proteins were then transferred by semi-dry electroblotting to nitrocellulose membranes (Amersham Protran 0.1 NC). The membrane was blocked for 30 min with 3% (w/v) dry non-fat milk in phosphate buffered saline (PBS) containing 0.1% Tween 20 and then incubated in primary antibody at room temperature. PBS was used to

dilute both primary and secondary antibodies. The membranes were washed in PBS containing 0.1% (v/v) Tween 20. Antibodies directed against CF_1 (1:40,000), OEE1 (oxygen evolving enhancer protein 1; 1:8,000), plastocyanin/Cyt c_6 (1:4,000), CTR3 (1:1,000) and CTR2 (1:1,000) (previously used in [7], CTR1 (1:1,000), FEA1/2 (1:20,000). The secondary antibody used was a goat anti-rabbit antibody (1:5,000 dilution) conjugated to alkaline phosphatase and processed according to the manufacturer's instructions.

Quantitative elemental analysis

Cell cultures corresponding to 1×10^8 cells (culture density of $3–5 \times 10^6$ cells/mL) were collected by centrifugation at 1424 x*g* for 3 min in a 50-mL falcon tube. The cells were washed twice in 50 mL of 1 mM Na_2EDTA pH 8.0 (to remove cell surface–associated metals) and once in Milli-Q water. The cell pellet was stored at −20°C before being overlaid with 286 µL 70% (v/v) nitric acid and digested at room temperature for 24 h and 65°C for about 2 h before being diluted to a final nitric acid concentration of 2% (v/v) with Milli-Q water. Complementary aliquots of fresh or spent culture medium were treated with nitric acid and brought to a final concentration of 2% (v/v) nitric acid. Metal, sulfur and phosphorus contents were determined by inductively coupled plasma mass spectrometry (ICP-MS/MS) on an Agilent 8800 Triple Quadropole ICP-MS instrument by comparison to an environmental calibration standard (Agilent 5183-4688), a sulfur (Inorganic Ventures CGS1) and phosphorus (Inorganic Ventures CGP1) standard. ^{89}Y served as an internal standard (Inorganic Ventures MSY-100PPM). The levels of analytes were determined in MS/MS mode. ^{23}Na, ^{24}Mg, ^{31}P, ^{55}Mn, ^{63}Cu and ^{66}Zn analytes were measured directly using He in a collision reaction cell. ^{39}K, ^{40}Ca and ^{56}Fe were directly determined using H_2 as a cell gas. The stable isotope of sulfur ^{32}S was determined via mass-shift from 32 to 48 utilizing O_2 as a cell gas and used as internal control. An average of four technical replicate measurements was used for each individual biological sample. The average variation between technical replicate measurements was 1.1% for all analytes and never exceeded 5% for an individual sample. Triplicate samples (from independent cultures) were also used to determine the variation between cultures. Averages and standard deviations between these replicates are shown in the figures.

Confocal microscopy using CS3 dye

CS3 dye was synthesized as described in Supplemental File 1. Cell-walled Chlamydomonas cells were cultured to early stationary phase and $1–2 \times 10^7$ cells very

collected by centrifugation at room temperature at 3,500 x*g*, for 2 min. The supernatant was discarded and the cell pellet was resuspended in 10 mM Na-phosphate buffer (pH 7.0) containing 10 µM CS3 dye. To avoid mechanical stress to cell wall-reduced cells, they were not centrifuged, but 10 µM CS3 dye was added directly to an aliquot of the culture instead. Microscopy was performed on a Zeiss LSM880. The following excitations and emissions were used: CS3 ex/em 514 nm/537 nm, chlorophyll 633 nm/696 nm. All aspects of image capture were controlled via Zeiss ZEN Black software, including fluorescent emission signals from probes and/or chlorophyll.

Statistical Analyses

Unless stated otherwise, a one-way ANOVA was used to test for differences between samples. Significance indicated by ANOVA was followed by a Holm-Sidak post-hoc test. Asterisks indicate a p-value of <0.05.

Bioinformatic analyses

The sequence similarity network (SSN) of the CTR family was constructed using the EFI-EST webtool (http://efi.igb.illinois.edu/efi-est/) [55] with an alignment score of 15; nodes were collapsed based on 70% sequence identity. Sequences for inclusion in the network were identified based on the presence of the CTR domain defined by IPR007274 from the InterPro database [56] or identified in a jackhammer search [57] using CTR3 as the query. The network was visualized with Cytoscape v3.10.1 using the Prefuse Force Directed OpenCL Layout. For the phylogenetic reconstruction, CTR1 and CTR3 protein sequences were used to search the UniProt database [58] with blastp. After manually filtering low-quality hits, 285 protein sequences were used to build an approximately maximum-likelihood phylogenetic tree with MAFFT [59] and FastTreeMP [60] and on the CIPRES Science Gateway [61] with default parameters. The resulting tree was visualized and annotated in iTol [62]. Branches with less than 0.5 bootstrap support were deleted. Precomputed AlphaFold predictions [63] were downloaded from the AlphaFold Protein Structure Database (https://alphafold.ebi.ac.uk/). Sequence logos were visualized with Skylign [64].

ACKNOWLEDGMENTS

The work was supported by a grant from the National Institutes of Health GM42143. Work at the Molecular Foundry was supported by the Office of Science, Office of Basic Energy Sciences, of the U.S. Department of Energy under Contract No. DE-AC02-05CH11231. Work at the U.S. Department of Energy Joint Genome Institute (https://ror.org/04xm1d337), a DOE Office of Science User Facility, is supported by

the Office of Science of the U.S. Department of Energy operated under Contract No. DE-AC02-05CH11231. Confocal microscopy experiments were conducted using a Zeiss LSM 880, at the CRL Molecular Imaging Center, supported by the Helen Wills Neuroscience Institute. We would like to thank Holly Aaron and Feather Ives for their microscopy training and assistance (RRID:SCR_017852), and Chris Jeans and the QB3 Macrolab at UC Berkeley for purification of LbCpf1.

AUTHOR CONTRIBUTIONS

Designed experiments: DS, SRS, Designed CS3 synthesis HN; Performed experiments: DS, SRS, SP, BCB, SG, CS, PAS, JLM; Analyzed data: DS, SRS, SP, SSM; Prepared figures: DS, SRS, SP, CBH; Designed project: DS, SSM; Secured funding: SSM. Wrote manuscript: DS, SSM.

CONFLICT OF INTEREST STATEMENT

The authors declare no conflict of interest.

DATA AVAILABILITY STATEMENT

The data underlying this article are available in the article and in its online supplementary material.

FIGURE LEGENDS

Figure 1: CRR1 is required for *CTR* gene expression and for Cu uptake. (A) *CTR1*, *CTR2* and *CTR3* mRNA abundances (in Fragments Per Kilobase of transcript per Million mapped reads - FPKMs) in Cu deficient c*rr1-2* (mutant) and *CRR1* (wildtype) grown as indicated, according to (Castruita et al. 2011). (B) Experimental design for Cu resupply experiments. Cells were grown in medium without Cu supplementation until early exponential growth. 2 µM Cu-EDTA was added at time 0. (C) ICP-MS/MS analysis at the indicated time points. Cu content, normalized to ^{32}S as a measure for biomass, before (−1 h) and after (0.5 h and 3 h) Cu addition. Shown are data points, averages and StDEV of three independent experiments.

Figure 2: Chlamydomonas CTR1, CTR2, and CTR3 belong to the CTRA-containing family. (A) Sequence similarity network on the CTR family and CTRA-containing proteins. Nodes are colored based on taxonomy according to the color key. The clusters to which the *Saccharomyces cerevisiae* (labeled with “Sc”), *Arabidopsis thaliana* (labeled with “At”), *Homo sapiens* (labeled with “Hs”), and the *Chlamydomonas reinhardtii* (labeled with “Cr”) CTR-family proteins belong are indicated with an arrow. The major distinct clusters and subclusters are delineated with a dotted line and labelled. The CTRA-containing cluster is outlined with a blue dotted

line, and a close-up view is provided in the blue square in the upper right of the panel. (B) Phylogenetic tree of proteins similar to CTR1, CTR2, and CTR3. The outer circle is used to indicate whether the leaf represents a protein with a CTR domain (without the CTRA domain), a CTRA-CTR fusion, or a CTRA-containing protein (without the CTR domain). The inner circle is used to convey taxonomic information for each leaf according the to the color key. The Chlorophyceae-specific clade containing *C. reinhardtii* CTR1, CTR2, and CTR3 is highlighted with thicker branches and the location of these proteins is labeled.

Figure 3: CTR dependent Cu uptake in Cu replete cultures. (A). Cu content from strains as indicated was determined by ICP-MS/MS. Black symbols and bars indicate the corresponding wild-type strains. Null mutants are indicated in white and a leaky mutant in grey as follows: *ctr1-1* (triangle up), *ctr1-2* (triangle down), *ctr1-3* (square), *ctr1-4* (circle), *ctr1-5* (diamond). Shown are data points, averages and StDEV of 3-9 independent experiments. (B) Relative transcript abundances of *CTR1* and *CTR2* were determined using quantitative RT-PCR. Cells were grown in Cu replete conditions. Samples collected from wild-type background strain (black triangle up), *ctr1* mutant lines (white triangle up). reference strain CC4533 (filled circles), *ctr2-2* (open, gray circles) and *ctr2-1* (open white circles). Each symbol represents an independent experiment.

Figure 4: Molecular analysis of *ctr* mutants and internal Cu deficiency in *ctr2*. (A) *ctr1-1, ctr2-1, ctr2-2, ctr3-1* and respective reference lines were grown photoheterotrophically under Cu-deficient (–) or Cu-replete (+) conditions. (A) Abundance of Plastocyanin and cytochrome c_6 was determined by separating 10 µg of total soluble cell lysate using SDS-PAGE (15% monomer), followed by immunoblotting using antisera cross-reactive to plastocyanin (PC, black arrow) and Cyt c_6 (white arrow). In order to check abundance of Cox2b, proteins in total cell lysates were separated by SDS-PAGE (15% monomer) followed by immunoblotting for CoxIIb. Either OEE1, alpha and beta subunits of CF_1, Ponceau S stain (Pon S) or Coomassie blue (CB) were used as loading controls. (B) Dilution series of (left panel) Cu deficient CC4533 to determine Cyt c_6 abundance and of (right panel) Cu replete CC4533 to determine plastocyanin abundance in *ctr2-1* and *ctr2*-2. Shown is one example from at least two independent experiments.

Figure 5: Although both CTR1 and CTR2 are up-regulated under poor Cu nutrition, only *ctr1* mutants recapitulate the Cu nutrition-dependent *crr1* phenotype. (A) *CTR1*, *CTR2* and *CTR3* mRNA abundances (in FPKM) in the Cu deficient wildtype strain CC1021 (Castruita et al. 2011). (B) Strains were grown photoheterotrophically under Cu-deficient (–) or Cu-replete (+) conditions. Pictures of flasks were taken six days post-inoculation.

Figure 6: CTR1 and CTR2 are both functional Cu importers *in vivo*, albeit with distinct functional properties. (ABDE) Cu addition experiment was performed as described in Figure 1. Cu content measured by ICP-MS/MS. Individual data points are shown with averages indicated by the bars and STDEV of 3-6 independent experiments. (CF) Relative transcript abundances of *CTR1* and *CTR2* were determined using quantitative RT-PCR. Data points, each representing an independent experiment, indicate the fold-difference in Cu-deficient vs. -replete medium.

Figure 7: Copper accumulation is impaired in zinc deficient *ctr1* and *ctr2* mutants. (A) Expression of *CTR1*, *CTR2* and *CTR3* is increased in Zn deficiency relative to sufficiency. RNA sequencing data from [46, 53]. (BCD) Cu content of *ctr1*, *ctr2* and *ctr3* mutants and corresponding reference strains grown in Zn deplete media, supplemented with Cu as indicated, was measured using ICP-MS/MS. Shown are data points, averages and StDEV of at least three independent experiments.

Figure 8: Excess Cu accumulates in Zn deficient *crr1* and is stored in acidocalcisomes, but cannot be mobilized after Zn add back. Cells were grown in copper replete medium, washed with 1 mM EDTA and resuspended in Zn deplete media as shown in (A). (B) Pictures of flasks were taken every 24 h during the experiment. (C) Cu content of *CRR1* and *crr1* cell lines was measured using ICP-MS/MS. Growth medium was supplied with either 1.2 µM (*CRR1*) or 40 µM Cu (*crr1*) to Zn-deplete growth medium as indicated. Shown are averages and individual data points of two independent experiments. (D) After 48 h in Zn deficiency, Zn was added back to the culture medium. Samples for imaging were taken right before and 7 h after Zn add back. Cu was visualized using the Cu(I) sensitive dye CS3 (red), cells were visualized using chlorophyll autoflourescence (green). Shown are max intensity projections of each channel. Scale bars represents 5 µm. Experiment was performed at least twice with independent cultures. At least 6 cells were imaged and are shown in Supplemental Figure 9.

Figure 9: CTR2 exports Cu(I) out of the acidocalcisomes. Cells were grown in medium without Zn supplementation. At a cell density between 2-4 x 10^6 cells/ml, Zn was added back to the culture media. Samples for imaging were taken right before and 7 h after Zn addition. Cu was visualized using the Cu(I) sensitive dye CS3, cells were visualized using chlorophyll autofluorescence. Scale bars represents 5 µm. Experiments were performed at least twice with independent cultures. At least 5 cells of two independent mutants were imaged and are shown in Supplemental Figures 10 and 11.

REFERENCES

1. Festa RA, Thiele DJ. Copper: An essential metal in biology. *Curr Biol* 2011;**21**(21):R877-R83. doi: DOI 10.1016/j.cub.2011.09.040
2. Foster AW, Osman D, Robinson NJ. Metal preferences and metallation. *The Journal of biological chemistry* 2014;**289**(41):28095-103. doi: 10.1074/jbc.R114.588145
3. Solioz M, Stoyanov JV. Copper homeostasis in *Enterococcus hirae*. *FEMS microbiology reviews* 2003;**27**(2-3):183-95. doi: 10.1016/S0168-6445(03)00053-6
4. Dancis A, Haile D, Yuan DS, Klausner RD. The Saccharomyces-Cerevisiae Copper Transport Protein (Ctr1p) - Biochemical, Characterization, Regulation by Copper, and Physiological-Role in Copper Uptake. *Journal of Biological Chemistry* 1994;**269**(41):25660-7
5. Kampfenkel K, Kushnir S, Babiychuk E, Inze D, Van Montagu M. Molecular characterization of a putative *Arabidopsis thaliana* copper transporter and its yeast homologue. *The Journal of biological chemistry* 1995;**270**(47):28479-86
6. Zhou B, Gitschier J. hCTR1: a human gene for copper uptake identified by complementation in yeast. *Proc Natl Acad Sci U S A* 1997;**94**(14):7481-6
7. Page MD, Kropat J, Hamel PP, Merchant SS. Two Chlamydomonas CTR copper transporters with a novel cys-met motif are localized to the plasma membrane and function in copper assimilation. *The Plant cell* 2009;**21**(3):928-43. doi: 10.1105/tpc.108.064907
8. Hill KL, Hassett R, Kosman D, Merchant S. Regulated copper uptake in *Chlamydomonas reinhardtii* in response to copper availability. *Plant physiology* 1996;**112**(2):697-704. doi: Doi 10.1104/Pp.112.2.697
9. Georgatsou E, Mavrogiannis LA, Fragiadakis GS, Alexandraki D. The yeast Fre1p/Fre2p cupric reductases facilitate copper uptake and are regulated by the copper-modulated Mac1p activator. *The Journal of biological chemistry* 1997;**272**(21):13786-92
10. Hassett R, Kosman DJ. Evidence for Cu(II) reduction as a component of copper uptake by *Saccharomyces cerevisiae*. *The Journal of biological chemistry* 1995;**270**(1):128-34
11. Wang HL, Du HM, Li HY, Huang Y, Ding JZ, Liu C, Wang N, Lan H, Zhang SZ. Identification and functional characterization of the ZmCOPT copper transporter family in maize. *Plos One* 2018;**13**(7). doi: ARTN e0199081

10.1371/journal.pone.0199081
12. Kim BE, Nevitt T, Thiele DJ. Mechanisms for copper acquisition, distribution and regulation. *Nat Chem Biol* 2008;**4**(3):176-85. doi: 10.1038/nchembio.72
13. Aller SG, Eng ET, De Feo CJ, Unger VM. Eukaryotic CTR copper uptake transporters require two faces of the third transmembrane domain for helix packing, oligomerization, and function. *The Journal of biological chemistry* 2004;**279**(51):53435-41. doi: 10.1074/jbc.M409421200
14. Puig S, Thiele DJ. Molecular mechanisms of copper uptake and distribution. *Current opinion in chemical biology* 2002;**6**(2):171-80
15. Peñarrubia L, Andrés-Colás N, Moreno J, Puig S. Regulation of copper transport in *Arabidopsis thaliana*: a biochemical oscillator? *Journal of biological inorganic chemistry : JBIC : a publication of the Society of Biological Inorganic Chemistry* 2010;**15**(1):29-36. doi: 10.1007/s00775-009-0591-8
16. Petris MJ. The SLC31 (Ctr) copper transporter family. *Pflugers Archiv : European journal of physiology* 2004;**447**(5):752-5. doi: 10.1007/s00424-003-1092-1
17. Turski ML, Thiele DJ. Drosophila Ctr1A functions as a copper transporter essential for development. *Journal of Biological Chemistry* 2007;**282**(33):24017-26. doi: 10.1074/jbc.M703792200
18. Zhou H, Cadigan KM, Thiele DJ. A copper-regulated transporter required for copper acquisition, pigmentation, and specific stages of development in *Drosophila melanogaster*. *The Journal of biological chemistry* 2003;**278**(48):48210-8. doi: 10.1074/jbc.M309820200
19. Logeman BL, Wood LK, Lee J, Thiele DJ. Gene duplication and neo-functionalization in the evolutionary and functional divergence of the metazoan copper transporters Ctr1 and Ctr2. *The Journal of biological chemistry* 2017;**292**(27):11531-46. doi: 10.1074/jbc.M117.793356
20. Ohrvik H, Nose Y, Wood LK, Kim BE, Gleber SC, Ralle M, Thiele DJ. Ctr2 regulates biogenesis of a cleaved form of mammalian Ctr1 metal transporter lacking the copper- and cisplatin-binding ecto-domain. *Proc Natl Acad Sci U S A* 2013;**110**(46):E4279-88. doi: 10.1073/pnas.1311749110
21. Sancenón V, Puig S, Mira H, Thiele DJ, Peñarrubia L. Identification of a copper transporter family in *Arabidopsis thaliana*. *Plant molecular biology* 2003;**51**(4):577-87. doi: Doi 10.1023/A:1022345507112

22. Sancenón V, Puig S, Mateu-Andres I, Dorcey E, Thiele DJ, Peñarrubia L. The Arabidopsis copper transporter COPT1 functions in root elongation and pollen development. *Journal of Biological Chemistry* 2004;**279**(15):15348-55. doi: 10.1074/jbc.M313321200
23. Garcia-Molina A, Andres-Colas N, Perea-Garcia A, Neumann U, Dodani SC, Huijser P, Penarrubia L, Puig S. The Arabidopsis COPT6 Transport Protein Functions in Copper Distribution Under Copper-Deficient Conditions. *Plant and Cell Physiology* 2013;**54**(8):1378-90. doi: 10.1093/pcp/pct088
24. Jung HI, Gayomba SR, Rutzke MA, Craft E, Kochian LV, Vatamaniuk OK. COPT6 is a plasma membrane transporter that functions in copper homeostasis in Arabidopsis and is a novel target of SQUAMOSA promoter-binding protein-like 7. *The Journal of biological chemistry* 2012;**287**(40):33252-67. doi: 10.1074/jbc.M112.397810
25. Andres-Colas N, Perea-Garcia A, Puig S, Penarrubia L. Deregulated copper transport affects Arabidopsis development especially in the absence of environmental cycles. *Plant physiology* 2010;**153**(1):170-84. doi: 10.1104/pp.110.153676
26. Klaumann S, Nickolaus SD, Furst SH, Starck S, Schneider S, Neuhaus HE, Trentmann O. The tonoplast copper transporter COPT5 acts as an exporter and is required for interorgan allocation of copper in *Arabidopsis thaliana*. *New Phytol* 2011;**192**(2):393-404. doi: 10.1111/j.1469-8137.2011.03798.x
27. Garcia-Molina A, Andres-Colas N, Perea-Garcia A, Del Valle-Tascon S, Penarrubia L, Puig S. The intracellular Arabidopsis COPT5 transport protein is required for photosynthetic electron transport under severe copper deficiency. *Plant J* 2011;**65**(6):848-60. doi: 10.1111/j.1365-313X.2010.04472.x
28. Andres-Colas N, Carrio-Segui A, Abdel-Ghany SE, Pilon M, Penarrubia L. Expression of the Intracellular COPT3-Mediated Cu Transport Is Temporally Regulated by the TCP16 Transcription Factor. *Front Plant Sci* 2018;**9**:910. doi: 10.3389/fpls.2018.00910
29. Hsieh SI, Castruita M, Malasarn D, Urzica E, Erde J, Page MD, Yamasaki H, Casero D, Pellegrini M, Merchant SS, Loo JA. The proteome of copper, iron, zinc, and manganese micronutrient deficiency in *Chlamydomonas reinhardtii*. *Mol Cell Proteomics* 2013;**12**(1):65-86. doi: 10.1074/mcp.M112.021840
30. Allen MD, del Campo JA, Kropat J, Merchant SS. FEA1, FEA2, and FRE1, encoding two homologous secreted proteins and a candidate ferrireductase, are

expressed coordinately with FOX1 and FTR1 in iron-deficient Chlamydomonas reinhardtii. *Eukaryotic cell* 2007;**6**(10):1841-52. doi: 10.1128/EC.00205-07
31. Merchant SS, Schmollinger S, Strenkert D, Moseley JL, Blaby-Haas CE. From economy to luxury: Copper homeostasis in Chlamydomonas and other algae. *Biochimica et biophysica acta Molecular cell research* 2020;**1867**(11):118822. doi: 10.1016/j.bbamcr.2020.118822
32. Merchant S, Bogorad L. Metal ion regulated gene expression: use of a plastocyanin-less mutant of *Chlamydomonas reinhardtii* to study the Cu(II)-dependent expression of cytochrome c-552. *EMBO J* 1987;**6**(9):2531-5. doi: 10.1002/j.1460-2075.1987.tb02540.x
33. Kropat J, Tottey S, Birkenbihl RP, Depege N, Huijser P, Merchant S. A regulator of nutritional copper signaling in Chlamydomonas is an SBP domain protein that recognizes the GTAC core of copper response element. *P Natl Acad Sci USA* 2005;**102**(51):18730-5. doi: 10.1073/pnas.0507693102
34. Strenkert D, Schmollinger S, Hu Y, Hofmann C, Holbrook K, Liu HW, Purvine SO, Nicora CD, Chen S, Lipton MS, Northen TR, Clemens S, Merchant SS. Zn deficiency disrupts Cu and S homeostasis in Chlamydomonas resulting in over accumulation of Cu and Cysteine. *Metallomics : integrated biometal science* 2023;**15**(7). doi: 10.1093/mtomcs/mfad043
35. Garcia-Santamarina S, Probst C, Festa RA, Ding C, Smith AD, Conklin SE, Brander S, Kinch LN, Grishin NV, Franz KJ, Riggs-Gelasco P, Lo Leggio L, Johansen KS, Thiele DJ. A lytic polysaccharide monooxygenase-like protein functions in fungal copper import and meningitis. *Nat Chem Biol* 2020;**16**(3):337-44. doi: 10.1038/s41589-019-0437-9
36. Xiao Z, Wedd AG. A C-terminal domain of the membrane copper pump Ctr1 exchanges copper(I) with the copper chaperone Atx1. *Chem Commun (Camb)* 2002(6):588-9. doi: 10.1039/b111180a
37. Honegger R. Lichens and Their Allies Past and Present. In: Scott B, Mesarich Cs (eds)*. Plant Relationships: Fungal-Plant Interactions*. Cham: Springer International Publishing, 2023, 133-83
38. Ferenczi A, Pyott DE, Xipnitou A, Molnár A. Efficient targeted DNA editing and replacement in *Chlamydomonas reinhardtii* using Cpf1 ribonucleoproteins and single-stranded DNA. *Proc Natl Acad Sci U S A* 2017;**114**(51):13567-72. doi: 10.1073/pnas.1710597114

39. Greiner A, Kelterborn S, Evers H, Kreimer G, Sizova I, Hegemann P. Targeting of Photoreceptor Genes in *Chlamydomonas reinhardtii* via Zinc-Finger Nucleases and CRISPR/Cas9. *The Plant cell* 2017;**29**(10):2498-518. doi: 10.1105/tpc.17.00659
40. Pham KLJ, Schmollinger S, Merchant SS, Strenkert D. Chlamydomonas ATX1 is essential for Cu distribution to multiple cupro-enzymes and maintenance of biomass in conditions demanding cupro-enzyme-dependent metabolic pathways. *Plant direct* 2022;**6**(2):e383. doi: 10.1002/pld3.383
41. Li XB, Patena W, Fauser F, Jinkerson RE, Saroussi S, Meyer MT, Ivanova N, Robertson JM, Yue R, Zhang R, Vilarrasa-Blasi J, Wittkopp TM, Ramundo S, Blum SR, Goh A, Laudon M, Srikumar T, Lefebvre PA, Grossman AR, Jonikas MC. A genome-wide algal mutant library and functional screen identifies genes required for eukaryotic photosynthesis. *Nat Genet* 2019;**51**(4):627-+. doi: 10.1038/s41588-019-0370-6
42. Liu J, Sitaram A, Burd CG. Regulation of copper-dependent endocytosis and vacuolar degradation of the yeast copper transporter, Ctr1p, by the Rsp5 ubiquitin ligase. *Traffic* 2007;**8**(10):1375-84. doi: 10.1111/j.1600-0854.2007.00616.x
43. Bremner I, Beattie JH. Copper and zinc metabolism in health and disease: speciation and interactions. *The Proceedings of the Nutrition Society* 1995;**54**(2):489-99. doi: 10.1079/pns19950017
44. Dainty SJ, Patterson CJ, Waldron KJ, Robinson NJ. Interaction between cyanobacterial copper chaperone Atx1 and zinc homeostasis. *Journal of biological inorganic chemistry : JBIC : a publication of the Society of Biological Inorganic Chemistry* 2010;**15**(1):77-85. doi: 10.1007/s00775-009-0555-z
45. Abdulla M. Copper levels after oral zinc. *Lancet* 1979;**1**(8116):616. doi: 10.1016/s0140-6736(79)91051-1
46. Hong-Hermesdorf A, Miethke M, Gallaher SD, Kropat J, Dodani SC, Chan J, Barupala D, Domaille DW, Shirasaki DI, Loo JA, Weber PK, Pett-Ridge J, Stemmler TL, Chang CJ, Merchant SS. Subcellular metal imaging identifies dynamic sites of Cu accumulation in Chlamydomonas. *Nat Chem Biol* 2014;**10**(12):1034-42. doi: 10.1038/nchembio.1662
47. Ravanel K, de Chassey B, Cornillon S, Benghezal M, Zulianello L, Gebbie L, Letourneur F, Cosson P. Membrane sorting in the endocytic and phagocytic pathway

of *Dictyostelium discoideum*. *European journal of cell biology* 2001;**80**(12):754-64. doi: 10.1078/0171-9335-00215
48. Long H, Fang J, Ye L, Zhang B, Hui C, Deng X, Merchant SS, Huang K. Structural and functional regulation of Chlamydomonas lysosome-related organelles during environmental changes. *Plant physiology* 2023;**192**(2):927-44. doi: 10.1093/plphys/kiad189
49. Kropat J, Gallaher SD, Urzica EI, Nakamoto SS, Strenkert D, Tottey S, Mason AZ, Merchant SS. Copper economy in Chlamydomonas: prioritized allocation and reallocation of copper to respiration vs. photosynthesis. *Proc Natl Acad Sci U S A* 2015;**112**(9):2644-51. doi: 10.1073/pnas.1422492112
50. Malasarn D, Kropat J, Hsieh SI, Finazzi G, Casero D, Loo JA, Pellegrini M, Wollman FA, Merchant SS. Zinc deficiency impacts CO_2 assimilation and disrupts copper homeostasis in *Chlamydomonas reinhardtii*. *The Journal of biological chemistry* 2013;**288**(15):10672-83. doi: 10.1074/jbc.M113.455105
51. Imlay JA. The Mismetallation of Enzymes during Oxidative Stress. *Journal of Biological Chemistry* 2014;**289**(41):28121-8. doi: 10.1074/jbc.R114.588814
52. Sommer F, Kropat J, Malasarn D, Grossoehme NE, Chen XH, Giedroc DP, Merchant SS. The CRR1 Nutritional Copper Sensor in Chlamydomonas Contains Two Distinct Metal-Responsive Domains. *The Plant cell* 2010;**22**(12):4098-113. doi: 10.1105/tpc.110.080069
53. Castruita M, Casero D, Karpowicz SJ, Kropat J, Vieler A, Hsieh SI, Yan W, Cokus S, Loo JA, Benning C, Pellegrini M, Merchant SS. Systems biology approach in Chlamydomonas reveals connections between copper nutrition and multiple metabolic steps. *The Plant cell* 2011;**23**(4):1273-92. doi: 10.1105/tpc.111.084400
54. Kropat J, Hong-Hermesdorf A, Casero D, Ent P, Castruita M, Pellegrini M, Merchant SS, Malasarn D. A revised mineral nutrient supplement increases biomass and growth rate in *Chlamydomonas reinhardtii*. *Plant J* 2011;**66**(5):770-80. doi: 10.1111/j.1365-313X.2011.04537.x
55. Gerlt JA, Bouvier JT, Davidson DB, Imker HJ, Sadkhin B, Slater DR, Whalen KL. Enzyme Function Initiative-Enzyme Similarity Tool (EFI-EST): A web tool for generating protein sequence similarity networks. *Bba-Proteins Proteom* 2015;**1854**(8):1019-37. doi: 10.1016/j.bbapap.2015.04.015
56. Paysan-Lafosse T, Blum M, Chuguransky S, Grego T, Pinto BL, Salazar GA, Bileschi ML, Bork P, Bridge A, Colwell L, Gough J, Haft DH, Letunic I, Marchler-

Bauer A, Mi H, Natale DA, Orengo CA, Pandurangan AP, Rivoire C, Sigrist CJA, Sillitoe I, Thanki N, Thomas PD, Tosatto SCE, Wu CH, Bateman A. InterPro in 2022. *Nucleic Acids Res* 2023;**51**(D1):D418-D27. doi: 10.1093/nar/gkac993

57. Finn RD, Clements J, Eddy SR. HMMER web server: interactive sequence similarity searching. *Nucleic Acids Res* 2011;**39**(Web Server issue):W29-37. doi: 10.1093/nar/gkr367

58. UniProt C. UniProt: the Universal Protein Knowledgebase in 2023. *Nucleic Acids Res* 2023;**51**(D1):D523-D31. doi: 10.1093/nar/gkac1052

59. Katoh K, Standley DM. MAFFT multiple sequence alignment software version 7: improvements in performance and usability. *Molecular biology and evolution* 2013;**30**(4):772-80. doi: 10.1093/molbev/mst010

60. Price MN, Dehal PS, Arkin AP. FastTree 2--approximately maximum-likelihood trees for large alignments. *Plos One* 2010;**5**(3):e9490. doi: 10.1371/journal.pone.0009490

61. Miller MA, Pfeiffer W, Schwartz T. Creating the CIPRES Science Gateway for inference of large phylogenetic trees. *2010 Gateway Computing Environments Workshop (GCE)*, 2010, 1-8

62. Letunic I, Bork P. Interactive Tree Of Life (iTOL) v5: an online tool for phylogenetic tree display and annotation. *Nucleic Acids Res* 2021;**49**(W1):W293-W6. doi: 10.1093/nar/gkab301

63. Jumper J, Evans R, Pritzel A, Green T, Figurnov M, Ronneberger O, Tunyasuvunakool K, Bates R, Zidek A, Potapenko A, Bridgland A, Meyer C, Kohl SAA, Ballard AJ, Cowie A, Romera-Paredes B, Nikolov S, Jain R, Adler J, Back T, Petersen S, Reiman D, Clancy E, Zielinski M, Steinegger M, Pacholska M, Berghammer T, Bodenstein S, Silver D, Vinyals O, Senior AW, Kavukcuoglu K, Kohli P, Hassabis D. Highly accurate protein structure prediction with AlphaFold. *Nature* 2021;**596**(7873):583-9. doi: 10.1038/s41586-021-03819-2

64. Wheeler TJ, Clements J, Finn RD. Skylign: a tool for creating informative, interactive logos representing sequence alignments and profile hidden Markov models. *Bmc Bioinformatics* 2014;**15**:7. doi: 10.1186/1471-2105-15-7

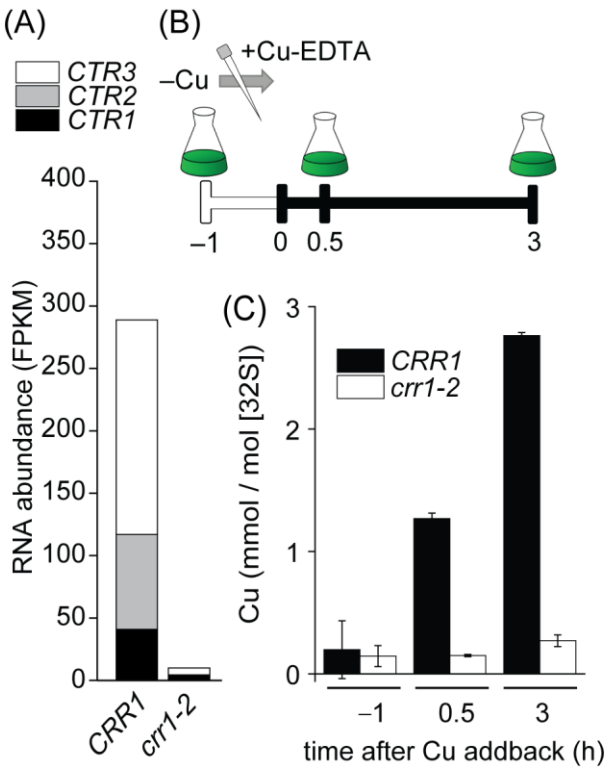

Figure 1: CRR1 is required for *CTR* gene expression and for Cu uptake. (A) *CTR1*, *CTR2* and *CTR3* mRNA abundances (in Fragments Per Kilobase of transcript per Million mapped reads - FPKMs) in Cu deficient c*rr1-2* (mutant) and *CRR1* (wildtype) grown as indicated, according to (Castruita et al. 2011). (B) Experimental design for Cu resupply experiments. Cells were grown in medium without Cu supplementation until early exponential growth. 2 µM Cu-EDTA was added at time 0. (C) ICP-MS/MS analysis at the indicated time points. Cu content, normalized to ^{32}S as a measure for biomass, before (−1 h) and after (0.5 h and 3 h) Cu addition. Shown are data points, averages and StDEV of three independent experiments.

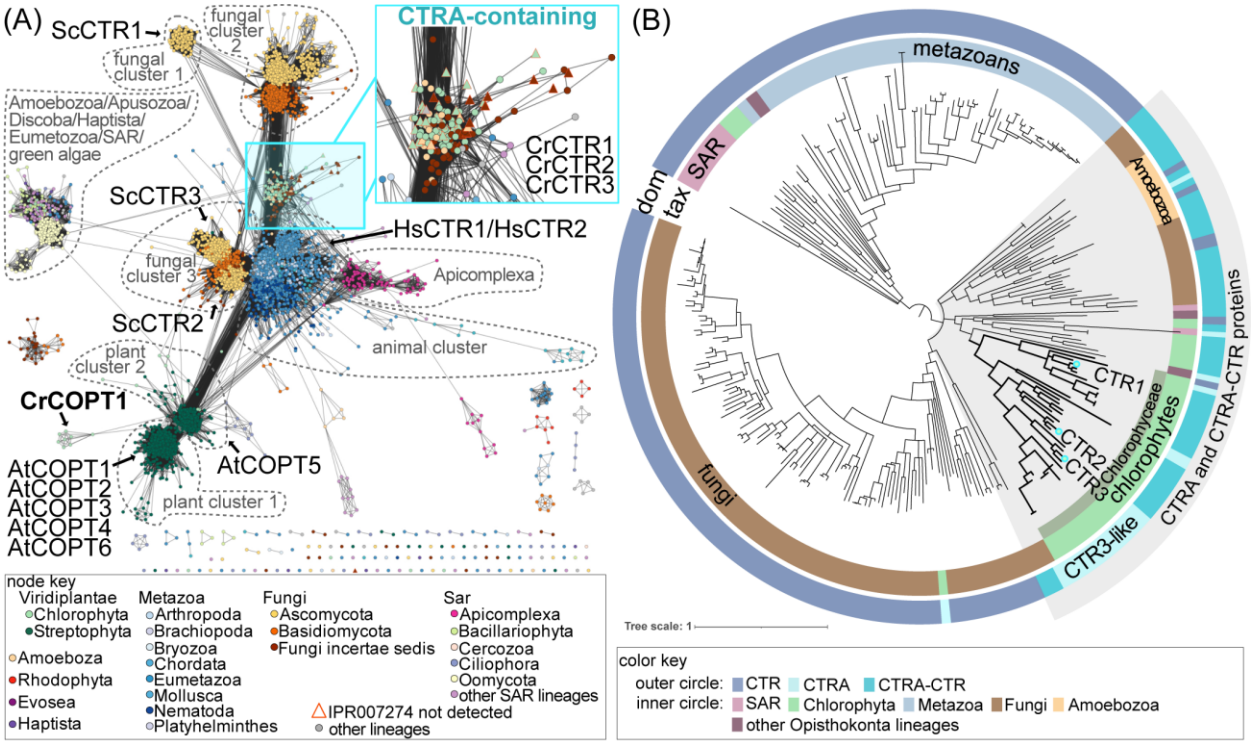

Figure 2: Chlamydomonas CTR1, CTR2, and CTR3 belong to the CTRA-containing family. (A) Sequence similarity network on the CTR family and CTRA-containing proteins. Nodes are colored based on taxonomy according to the color key. The clusters to which the *Saccharomyces cerevisiae* (labeled with "Sc"), *Arabidopsis thaliana* (labeled with "At"), *Homo sapiens* (labeled with "Hs"), and the *Chlamydomonas reinhardtii* (labeled with "Cr") CTR-family proteins belong are indicated with an arrow. The major distinct clusters and subclusters are delineated with a dotted line and labelled. The CTRA-containing cluster is outlined with a blue dotted line, and a close-up view is provided in the blue square in the upper right of the panel. (B) Phylogenetic tree of proteins similar to CTR1, CTR2, and CTR3. The outer circle is used to indicate whether the leaf represents a protein with a CTR domain (without the CTRA domain), a CTRA-CTR fusion, or a CTRA-containing protein (without the CTR domain). The inner circle is used to convey taxonomic information for each leaf according the to the color key. The Chlorophyceae-specific clade containing *C. reinhardtii* CTR1, CTR2, and CTR3 is highlighted with thicker branches and the location of these proteins is labeled.

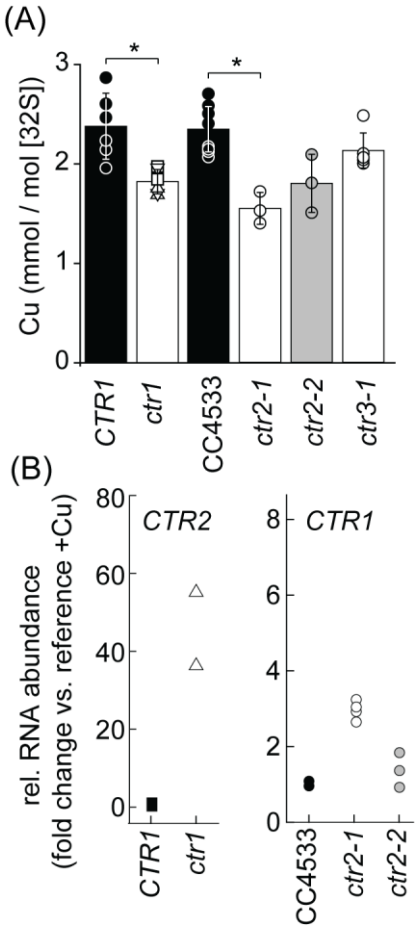

Figure 3: CTR dependent Cu uptake in Cu replete cultures. (A). Cu content from strains as indicated was determined by ICP-MS/MS. Black symbols and bars indicate the corresponding wild-type strains. Null mutants are indicated in white and a leaky mutant in grey as follows: *ctr1-1* (triangle up), *ctr1-2* (triangle down), *ctr1-3* (square), *ctr1-4* (circle), *ctr1-5* (diamond). Shown are data points, averages and StDEV of 3-9 independent experiments. (B) Relative transcript abundances of *CTR1* and *CTR2* were determined using quantitative RT-PCR. Cells were grown in Cu replete conditions. Samples collected from wild-type background strain (black triangle up), *ctr1* mutant lines (white triangle up). Reference strain CC4533 (filled circles), *ctr2-2* (open, gray circles) and *ctr2-1* (open white circles). Each symbol represents an independent experiment.

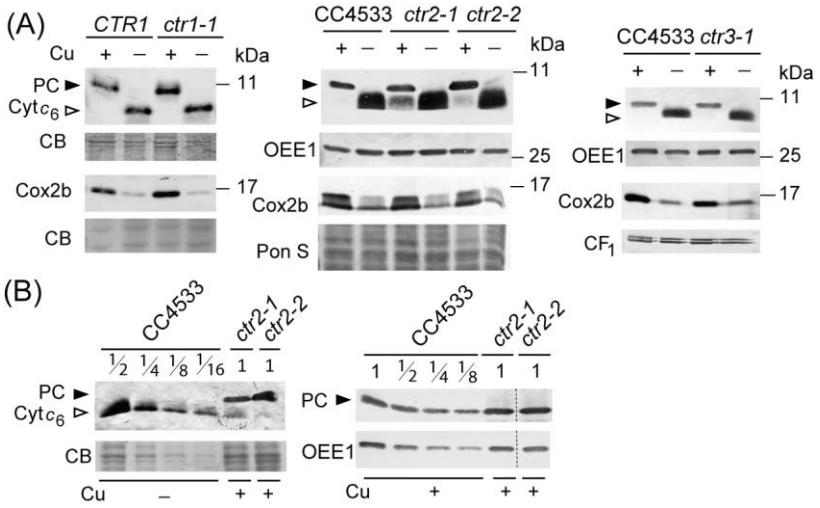

Figure 4: Molecular analysis of *ctr* mutants and internal Cu deficiency in *ctr2*. (A) *ctr1-1, ctr2-1, ctr2-2, ctr3-1* and respective reference lines were grown photoheterotrophically under Cu-deficient (–) or Cu-replete (+) conditions. (A) Abundance of Plastocyanin and cytochrome c_6 was determined by separating 10 µg of total soluble cell lysate using SDS-PAGE (15% monomer), followed by immunoblotting using antisera cross-reactive to plastocyanin (PC, black arrow) and Cyt c_6 (white arrow). In order to check abundance of Cox2b, proteins in total cell lysates were separated by SDS-PAGE (15% monomer) followed by immunoblotting for CoxIIb. Either OEE1, alpha and beta subunits of CF_1, Ponceau S stain (Pon S) or Coomassie blue (CB) were used as loading controls. (B) Dilution series of (left panel) Cu deficient CC4533 to determine Cyt c_6 abundance and of (right panel) Cu replete CC4533 to determine plastocyanin abundance in *ctr2-1* and *ctr2*-2. Shown is one example from at least two independent experiments.

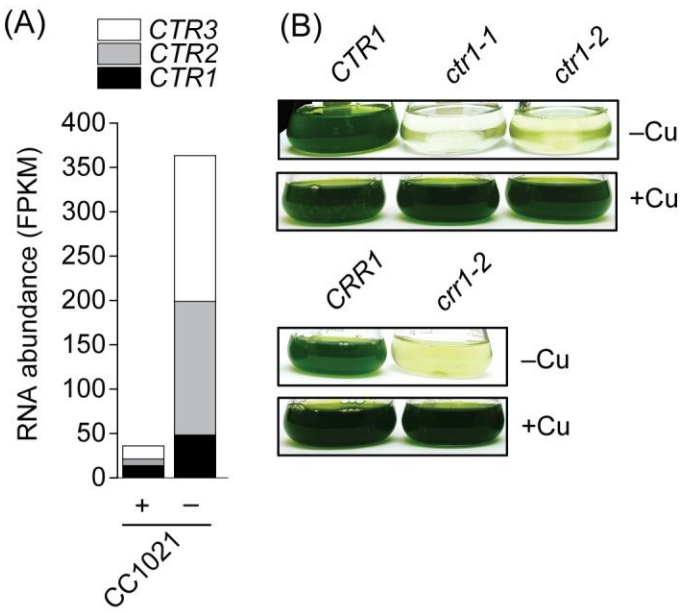

Figure 5: Although both CTR1 and CTR2 are up-regulated under poor Cu nutrition, only *ctr1* mutants recapitulate the Cu nutrition-dependent *crr1* phenotype. (A) *CTR1*, *CTR2* and *CTR3* mRNA abundances (in FPKM) in the Cu deficient wildtype strain CC1021 (Castruita et al. 2011). (B) Strains were grown photoheterotrophically under Cu-deficient (–) or Cu-replete (+) conditions. Pictures of flasks were taken six days post-inoculation.

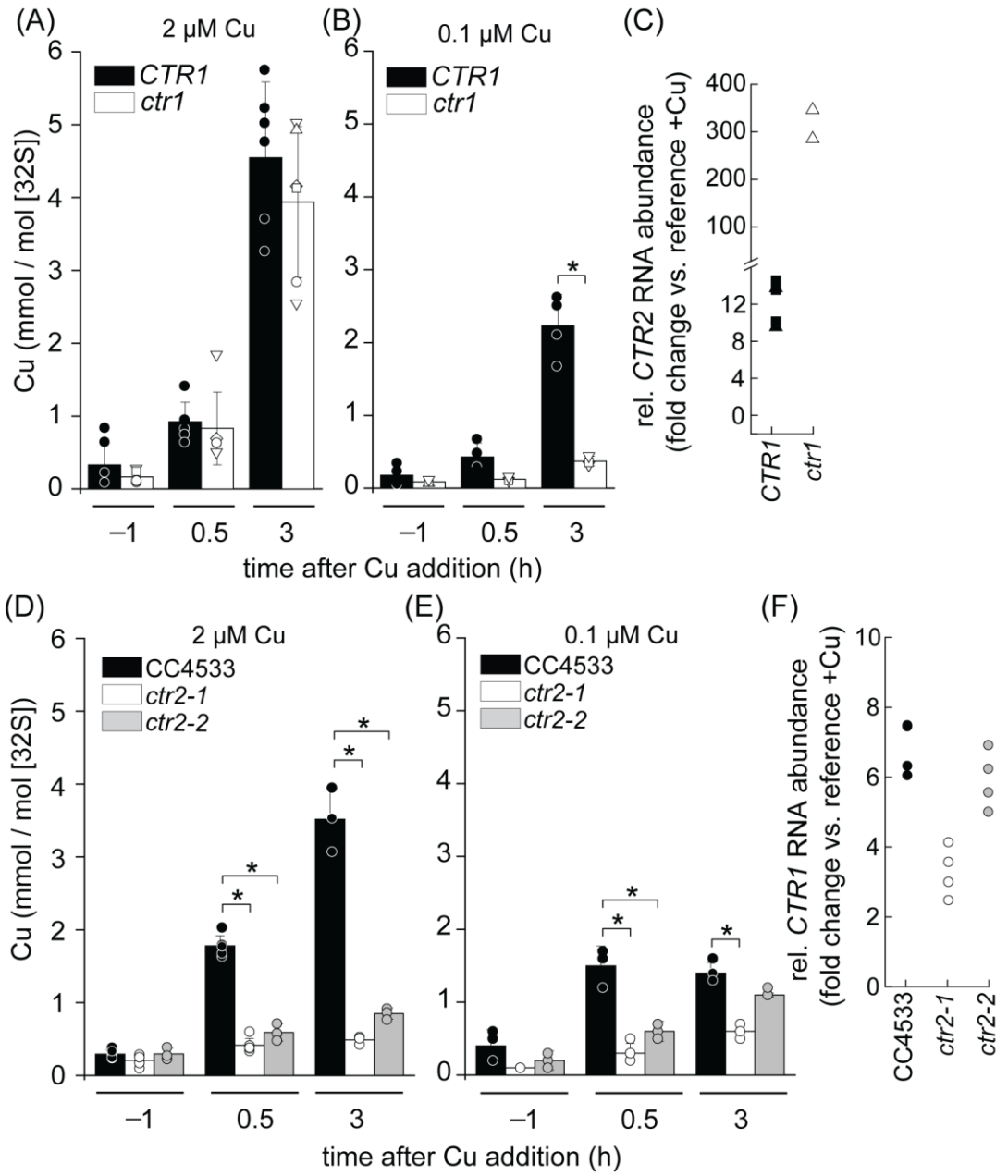

Figure 6: CTR1 and CTR2 are both functional Cu importers *in vivo*, albeit with distinct functional properties. (ABDE) Cu addition experiment was performed as described in Figure 1. Cu content measured by ICP-MS/MS. Individual data points are shown with averages indicated by the bars and STDEV of 3-6 independent experiments. (CF) Relative transcript abundances of *CTR1* and *CTR2* were determined using quantitative RT-PCR. Data points, each representing an independent experiment, indicate the fold-difference in Cu-deficient vs. -replete medium.

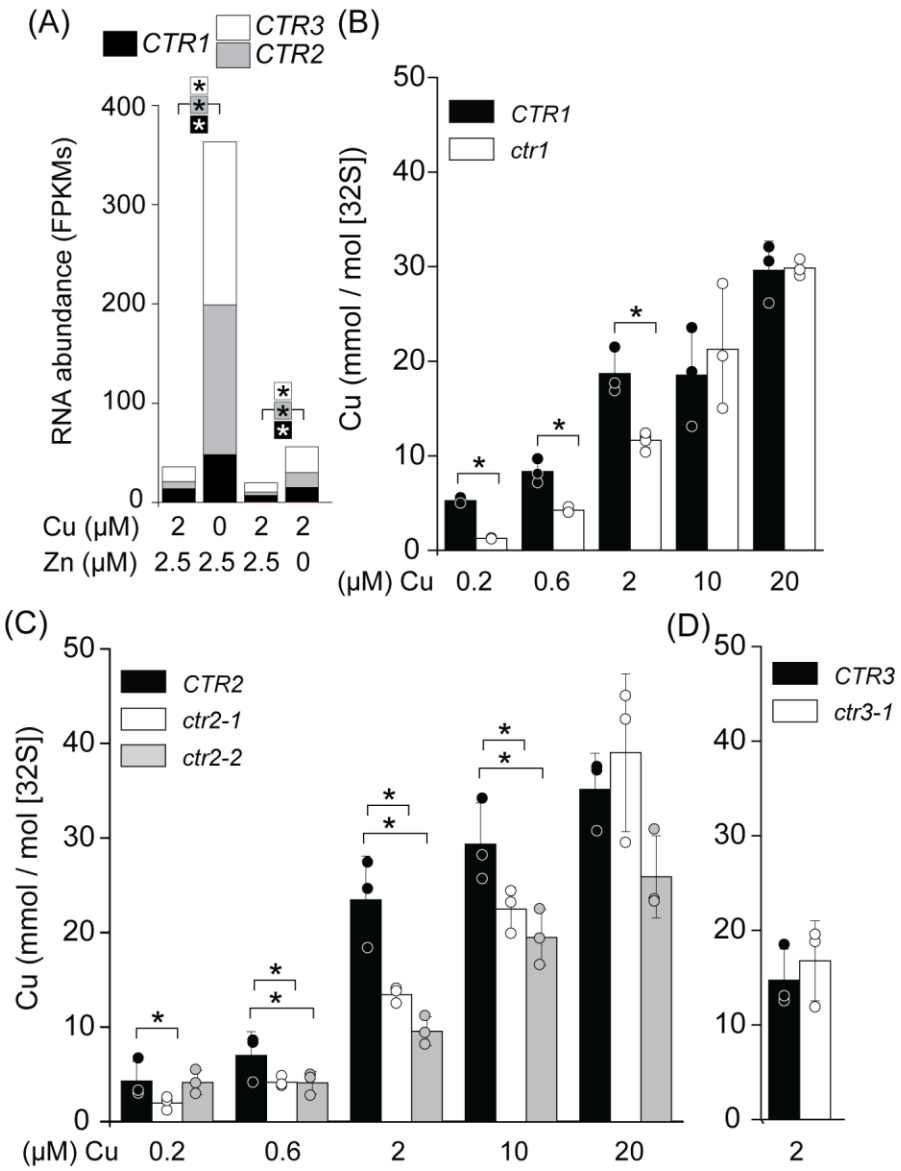

Figure 7: Copper accumulation is impaired in zinc deficient *ctr1* and *ctr2* mutants. (A) Expression of *CTR1*, *CTR2* and *CTR3* is increased in Zn deficiency relative to sufficiency. RNA sequencing data from (Castruita et al., 2011; Hong-Hermesdorf et al., 2014). (BCD) Cu content of *ctr1*, *ctr2* and *ctr3* mutants and corresponding reference strains grown in Zn deplete media, supplemented with Cu as indicated, was measured using ICP-MS/MS. Shown are data points, averages and StDEV of at least three independent experiments.

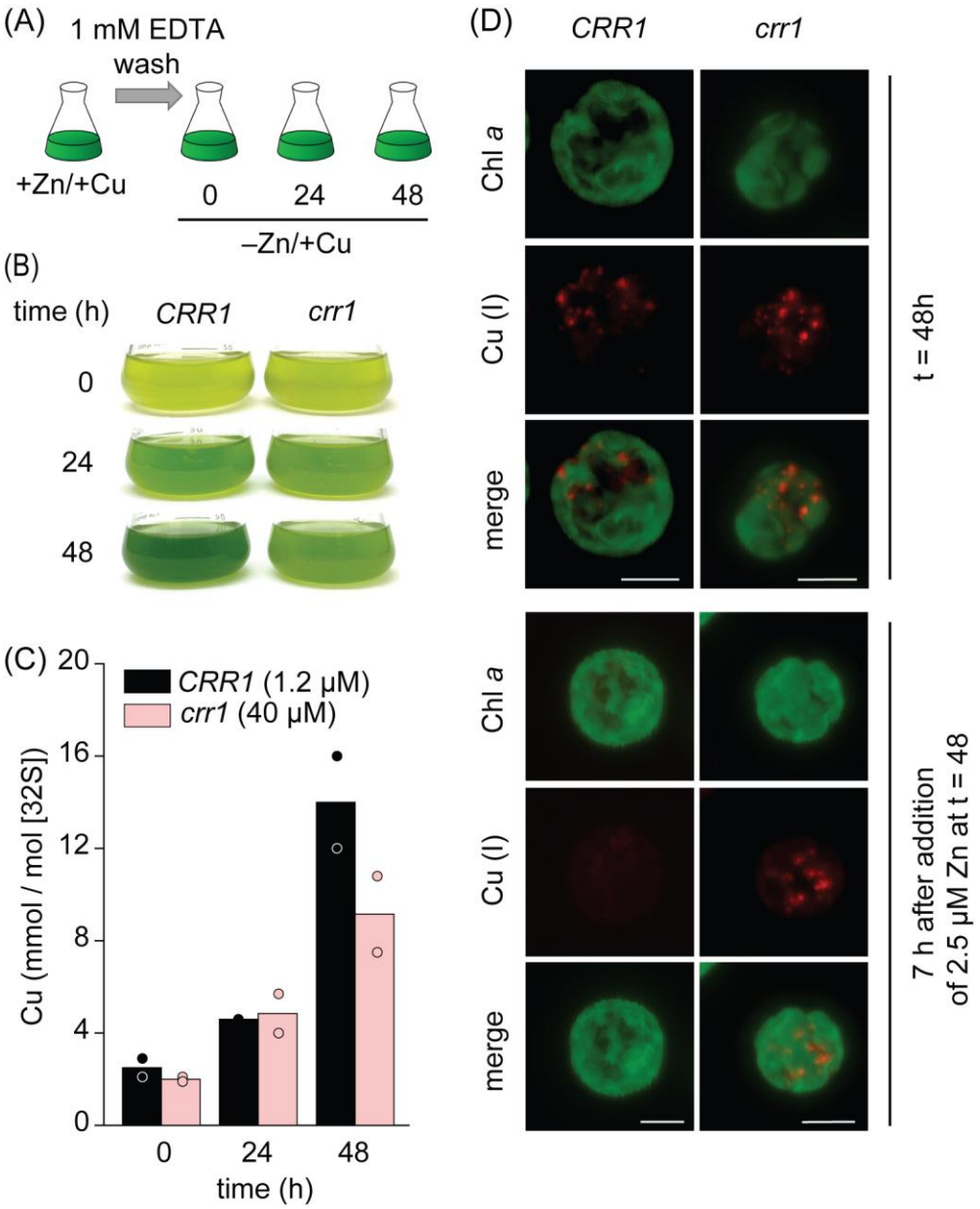

Figure 8: Excess Cu accumulates in Zn deficient *crr1* and is stored in acidocalcisomes, but cannot be mobilized after Zn add back. Cells were grown in copper replete medium, washed with 1 mM EDTA and resuspended in Zn deplete media as shown in (A). (B) Pictures of flasks were taken every 24 h during the experiment. (C) Cu content of *CRR1* and *crr1* cell lines was measured using ICP-MS/MS. Growth medium was supplied with either 1.2 µM (*CRR1*) or 40 µM Cu (*crr1*) to Zn-deplete growth medium as indicated. Shown are averages and individual data points of two independent experiments. (D) After 48 h in Zn deficiency, Zn was added back to the culture medium. Samples for imaging were taken right before and 7 h after Zn add back. Cu was visualized using the Cu(I) sensitive dye CS3 (red), cells were visualized using chlorophyll autoflourescence (green). Shown are max intensity projections of each channel. Scale

bars represents 5 µm. Experiment was performed at least twice with independent cultures. At least 6 cells were imaged and are shown in Supplemental Figure 9.

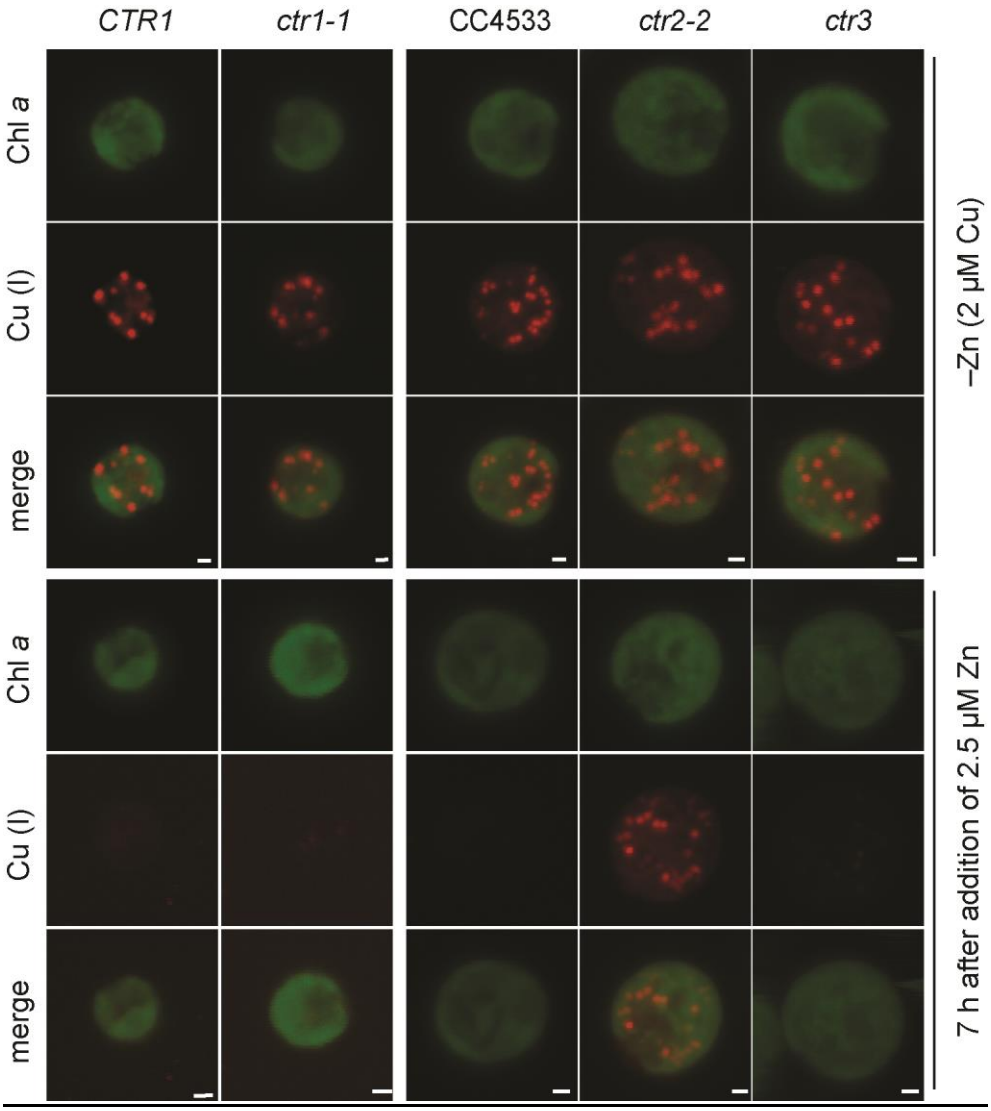

Figure 9: CTR2 exports Cu(I) out of the acidocalcisomes. Cells were grown in medium without Zn supplementation. At a cell density between 2-4 x 10^6 cells/ml, Zn was added back to the culture media. Samples for imaging were taken right before and 7 h after Zn addition. Cu was visualized using the Cu(I) sensitive dye CS3, cells were visualized using chlorophyll autofluorescence. Scale bars represents 5 µm. Experiments were performed at least twice with independent cultures. At least 5 cells of two independent mutants were imaged and are shown in Supplemental Figures 10 and 11.